a sterically compressed five-coordinate state by the macrocyclic ligand and that this stress or tension is released upon oxidation to Ni(III), as shown in **4b**. It should be noted that the replacement of the axial N donor atom of dioxo[16]aneN_5 by a weaker σ-donor S atom or a nondonor CH_2 group leaves only the strong square-planar ligand field to render the chelated Ni(II) into the low-spin state.[20] In other words, the axial donor N7 of the macrocyclic ligand determines the high-spin state of the enclosed Ni(II). The elongated high-spin Ni–equatorial N bond distances push the Ni(II) ion above the mean plane of the N_4 group and compel it to come closer to the axial donor N7 than normally permitted. The unusually short apical Ni(II)–N interaction would drive one unpaired d_{z^2} electron of the high-spin Ni(II) to the opposite trans side and labilize the other axial bond, as clearly shown by the lack of a ligand at the sixth coordination site in the **2a** crystal structure.

Unlike nucleophilic ligands (e.g. H_2O, halogen), the electrophilic ligand O_2 (tending to the form O_2^-) is likely to approach the vacant, "electron-rich" (by the N7 trans effect) sixth site of **2a**. The high-spin state of Ni(II) ($S = 1$) may smooth the way for interaction with the triplet state of O_2. Upon interaction with O_2, the Ni(II) ion that is liable for oxidation could partially transfer an electron to the bound O_2. Earlier, we proposed the 1:1 O_2 adducts as having a Ni(III)–O_2^- bond character mainly on the basis of the visible spectra that are similar to those of Ni(III) complexes.[20] As shown by the crystal structure of the Ni(III) complex **4b**, such electron release will diminish strain imposed by the macrocyclic ligand.

Since O_2 is a good π-acceptor, its coordination would demand an increase in N→Ni σ-donation to help compensate for the Ni→O_2 π-back-bond. In Scheme II, the deprotonated amides possibly act as "electron sinks" and can modify their π-donor characteristics toward the Ni ion via the sp^2 N^- donor atoms. A similar cis effect has been reported in coordination of CO to iron–porphyrin complexes.[34]

Supplementary Material Available: Listings of complete atomic coordinates and anisotropic thermal parameters and mean-square displacement tensors for non-hydrogen atoms for **2a** and **4b** and figures showing *a* axis and (010) projections for **4b** (14 pages); listings of observed and calculated structure factor amplitudes for **2a** and **4b** (27 pages). Ordering information is given on any current masthead page.

(34) James, B. R.; Sams, J. R.; Tsin, T. B.; Reimer, K. J. *J. Chem. Soc., Chem. Commun.* **1978**, 746.

Contribution from the Chemistry Department, University of Otago, Dunedin, New Zealand, and The Research School of Chemistry, The Australian National University, Canberra, ACT 2601, Australia

Cobalt(III)-Promoted Hydrolysis of Esters. Hydrolysis of Chelated and Monodentate β-Alanine Isopropyl Ester and Interconversions via Hydrolysis Intermediates

E. Baraniak,[‡] D. A. Buckingham,*[†] C. R. Clark,[†] B. H. Moynihan,[†] and A. M. Sargeson[‡]

Received February 18, 1986

Hydrolysis of isopropyl β-alaninate in the six-membered ester chelate $[Co(en)_2(\beta\text{-alaO-}i\text{-Pr})]^{3+}$ occurs by solvolytic attack at the directly activated carbonyl center with C–O-*i*-Pr bond fission to give chelated $[Co(en)_2(\beta\text{-alaO})]^{2+}$. Rate data ($I = 1.0$ mol dm^{-3} ($NaClO_4$), 25.0 °C) lead to the rate law $k_{obsd} = k[H_2O] + (k^I[OH^-] + k^{II}[OH^-]^2)/(1 + K[OH^-])$ with $k_{H_2O} = 8.3 \times 10^{-7}$ mol^{-1} dm^3 s^{-1} ($k_{H_2O}/k_{D_2O} = 2.5$), $k^I = 5.0 \times 10^3$ mol^{-1} dm^3 s^{-1} ($k^I_{H_2O}/k^I_{D_2O} = 0.89$), $k^{II} = 7.0 \times 10^8$ mol^{-2} dm^6 s^{-1} ($k^{II}_{H_2O}/k^{II}_{D_2O} = 0.74$), and $K = 1.75 \times 10^4$ mol^{-1} dm^3. This is interpreted as rate-determining H_2O and HO^- addition to the chelated ester at low and high pH, respectively, and rate-determining proton abstraction from an addition intermediate in the pH range 7–10. Catalysis by HPO_4^{2-}, imidazole, *N*-methylimidazole, ethyl glycinate, and HCO_3^- occurs ($k_{obsd} = k_B[B]$) with k_B values of 30, 8, 6, 3, and 40 mol^{-1} dm^3 s^{-1}, respectively. The HCO_3^--catalyzed reaction results in both hydrolysis to $[Co(en)_2(\beta\text{-alaO})]^{2+}$ with retention of the chelate ring (60%) and CoO–C chelate ring cleavage giving *cis*-$[Co(en)_2(OH)(\beta\text{-alaO-}i\text{-Pr})]^{2+}$ (40%). CO_2 reacts with the latter species in a rapid subsequent reaction ($k_{CO_2} = 580$ mol^{-1} dm^3 s^{-1}) forming *cis*-$[Co(en)_2(OCO_2)(\beta\text{-alaO-}i\text{-Pr})]^+$. Hydrolysis of the nonactivated monodentate ester in *cis*-$[Co(en)_2(OH_2)(\beta\text{-alaO-}i\text{-Pr})]^{3+}$ ($pK_a = 6.05 \pm 0.05$) and in *cis*-$[Co(en)_2(OH)(\beta\text{-alaO-}i\text{-Pr})]^{2+}$ occurs intramolecularly by attack of coordinated water and hydroxide, respectively, to give largely $[Co(en)_2(\beta\text{-alaO})]^{2+}$. The former reaction is slow ($k_{obsd} = 1.8 \times 10^{-6}$ s^{-1}, $I = 1.0$ mol dm^{-3} ($NaClO_4$), 25.0 °C), occurs with no ^2H isotope effect, and is accompanied by water exchange at the metal center ($k_{ex} = 1.5 \times 10^{-5}$ s^{-1}). The hydroxo complex follows the rate law $k_{obsd} = k_0 + k_{OH}[OH^-] + k_B[B]$ with $k_0 = (5.6 \pm 0.5) \times 10^{-6}$ s^{-1}, $k_{OH} = (0.22 \pm 0.02)$ mol^{-1} dm^3 s^{-1}, and k_B values following a Brønsted relationship ($\beta \sim 0.4$) with the exception of CO_3^{2-} and PO_4^{3-}, which show enhanced catalysis. Proton transfer from coordinated hydroxide to the catalyzing base plays an important part in this cyclization, which is rate-determining. Trapping experiments using glycine ethyl ester show that hydrolysis in the monodentate and chelated ester complexes occurs via a common intermediate.

Introduction

Several years ago we described the hydrolysis of Co(III)-chelated glycine esters (I) in which the metal directly activated the acyl function toward H_2O and OH^- attack (eq 1).[1,2] The

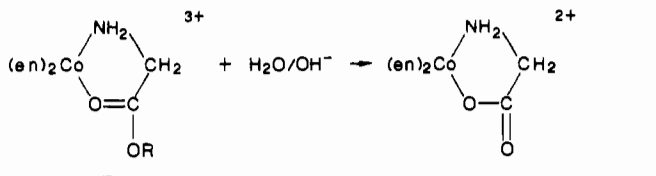

I

+ ROH (1)

10^6–10^7 fold increase in rate over that for the uncoordinated ester, as well as the rate difference between OH^- and H_2O (10^{11}), was shown to result from positive $\Delta S^\ddagger$ contributions. However, whether addition of the solvolytic component or elimination of RO^- was rate-determining was not established; the hydrolysis process could be concerted. Other O and N nucleophiles were shown to add rapidly to the activated carbonyl center,[2] and in Me_2SO the addition intermediate formed by using a primary amine nucleophile was directly observed.[3]

Attempts to follow the alternative hydrolysis pathway involving intramolecular attack by coordinated water or hydroxide on the essentially unactivated ester (II) were thwarted by our inability to isolate these complexes. Formation of the aqua reactant via

[†] University of Otago.
[‡] The Australian National University.

(1) Buckingham, D. A.; Foster, D. M.; Sargeson, A. M. *J. Am. Chem. Soc.* **1968**, *90*, 6032.
(2) Buckingham, D. A.; Foster, D. M.; Sargeson, A. M. *J. Am. Chem. Soc.* **1970**, *92*, 5701.
(3) Buckingham, D. A.; Dekkers, J.; Sargeson, A. M. *J. Am. Chem. Soc.* **1973**, *95*, 4173.

0020-1669/86/1325-3466$01.50/0

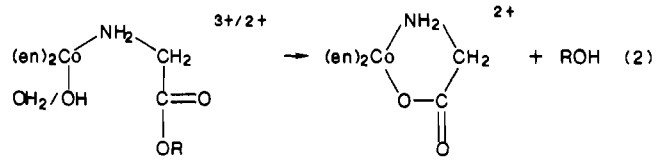

II

HOCl induced oxidation of coordinated bromide (eq 3) was implied by competition experiments, but it appeared to rapidly form chelate I by displacement of coordinated water.[1,4] Formation of the hydroxo reactant (eq 4) was demonstrated by ^{18}O tracer experiments, but intramolecular hydrolysis in it was too rapid to be seen as a separate process being camouflaged by its synthesis.[5]

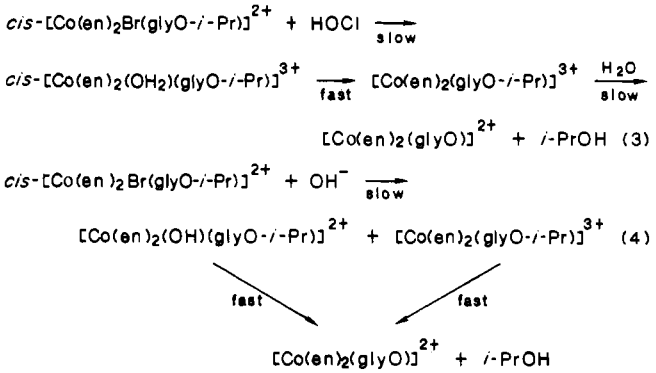

We have now been able to isolate and study separately the hydrolysis of the related amino acid ester, β-alanine isopropyl ester, as the chelate (III), as the cis aqua complex (IV), and as the cis hydroxo complex (V).

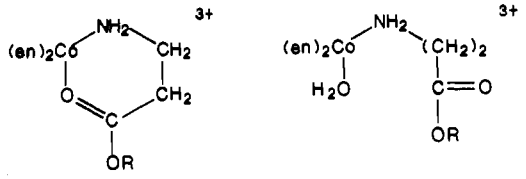

III

IV

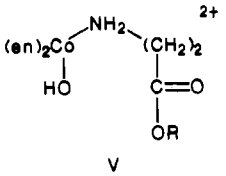

V

The synthesis and reactivity of these isolated species is now described and compared with the glycine chemistry.

Experimental Section

Visible spectra were recorded on Cary 14 or 219 spectrophotometers, and IR spectra on a Perkin-Elmer 459 spectrophotometer. ^1H and ^{13}C NMR were recorded on JEOL JNM-100 MHz or Varian FX-60 and EM-390 spectrometers. Co estimations were made spectrally with known molar absorptivities (ϵ, mol^{-1} dm^3 cm^{-1}) or by atomic absorption (AA).

Preparations. $[Co(en)_2(\beta\text{-alaOR})](ClO_4)_3$ (R = Me, *i*-Pr). To *cis*-$[Co(en)_2Br(\beta\text{-alaOR})]Br_2$[6] (22 g) suspended in dry acetone (25 cm^3) was added finely divided $AgClO_4$ (32 g) and the mixture kept in the dark for 1 h. Following removal of AgBr dry ether was added to separate the product as a red sticky mass, which was twice redissolved in dry acetone, filtered, and reprecipitated as an orange powder from dry Et_2O. This material was recrystallized after rapid dissolution in the minimum volume of warm water, addition of $NaClO_4$, and cooling in ice. Anal. Calcd for $[Co(en)_2(\beta\text{-alaOMe})](ClO_4)_3$: C, 16.55; H, 4.34; N, 12.06. Found: C, 17.0; H, 4.4; N, 11.8. Calcd for $[Co(en)_2(\beta\text{-alaO-}i\text{-Pr})](ClO_4)_3$: Co, 9.68; C, 19.72; H, 4.80; N, 11.51. Found: Co, 9.6; C, 19.8; H, 4.9; N, 11.3. Aqueous solutions of both complexes (0.1 mol dm^{-3} HCl or 1.0 mol dm^{-3} $NaClO_4$) gave ϵ_{492}(max) 98 ± 2 and ϵ_{348}(max) 70 ± 2. ^1H NMR: *gem*-CH_3 (doublet) 1.76 ppm (J = 6 Hz). IR: 1600 cm^{-1} (s, ester C=O).

***cis*-$[Co(en)_2(OH_2)(\beta\text{-alaO-}i\text{-Pr})](NO_3)_2(ClO_4)$.** To a suspension of *cis*-$[Co(en)_2Br(\beta\text{-alaO-}i\text{-Pr})]Br_2$ (38.5 g) in water (50 cm^3) was added 45.5 g of HgO dissolved in 37 cm^3 of 70% $HClO_4$. The mixture was shaken until the reactant had dissolved and then allowed to stand for 20 min. After cooling in ice and filtration to remove $HgBr_2$, a large excess of $LiNO_3$ and $LiClO_4$ was added, and then a 50-fold excess of EtOH containing a little MeOH added slowly while scratching the side of the glass vessel. An orange granular product slowly formed. This was collected and recrystallized from a minimum volume of water until ^1H NMR showed the absence of any chelate. Anal. Calcd for $[Co(en)_2(OH_2)(\beta\text{-alaO-}i\text{-Pr})](NO_3)_2(ClO_4)$: C, 21.77; H, 5.66; N, 17.77. Found: C, 21.7; H, 5.8; N, 17.9. An aqueous solution gave ϵ_{489}(max) 77 ± 2 and ϵ_{351}(max) 73 ± 2. ^1H NMR: *gem*-CH_3(doublet) 1.71 ppm (J = 6 Hz). The pK_a of the coordinated water molecule was determined by potentiometric titration (0.2 g in 10 cm^3 1.0 mol dm^{-3} $NaClO_4$) and by recording visible spectra as a function of pH.

***cis*-$[Co(en)_2(OCO_2)(\beta\text{-alaO-}i\text{-Pr})]ClO_4$.** To *cis*-$[Co(en)_2(OH_2)(\beta\text{-alaO-}i\text{-Pr})](NO_3)_3$ (0.79 g), suspended in warm water (3 cm^3), was slowly added Li_2CO_3 (0.11 g). The complex dissolved to give a wine red solution. Further Li_2CO_3 (0.11 g) was added after 10 min. and then solid CO_2, and finally methanol (10 cm^3). The solution was filtered and excess $NaClO_4 \cdot H_2O$ (3 g) and MeOH (20 cm^3) added to the filtrate, which was stored in the refrigerator overnight. The fine mauve red product was removed, washed with a little MeOH and ether, and air-dried. Anal. Calcd for $[Co(en)_2(OCO_2)(\beta\text{-alaO-}i\text{-Pr})]ClO_4$: C, 28.12; H, 6.22; N, 14.91. Found: C, 28.7; H, 6.0; N, 15.1. An aqueous solution gave ϵ_{500}(max) 123. In aqueous acid, the visible and ^1H NMR spectra of *cis*-$[Co(en)_2(H_2O)(\beta\text{-alaO-}i\text{-Pr})]^{3+}$ are reproduced.

Kinetics. Rate data at high pH were obtained on a Cary 16K or 219 spectrophotometer fitted with a thermostated Teflon cell (3.2 cm) with pH-stat control and under a N_2 atmosphere or by using a Durrum D-110 stopped-flow spectrophotometer. Consumption of OH^- vs. time was recorded with the pH-stat apparatus, and reaction products were analyzed by AA and by comparisons of their absorption spectra with those of authentic complexes following separation on Bio-Rad analytical Dowex 50W-X2 (200–400 mesh, H^+ or Na^+ form) cation-exchange resin. Following alkaline hydrolysis of the *cis*-$[Co(en)_2(OH)(\beta\text{-alaO-}i\text{-Pr})]^{2+}$ ion, the mauve and cerise 1+ products were separated and eluted with 0.5 mol dm^{-3} $NaClO_4$ (pH 9) and $[Co(en)_2(\beta\text{-alaO})]^{2+}$ was eluted with 2 mol dm^{-3} $NaClO_4$ (pH 8).

Reaction Products. Products of the HCO_3^--induced reaction of $[Co(en)_2(\beta\text{-alaO-}i\text{-Pr})](ClO_4)_3$ (Table XIV) were determined as follows. To 40–70 mg of complex were added 10-cm^3 mixtures of 1.0 mol dm^{-3} $NaHCO_3$ (freshly made up) and 1.0 mol dm^{-3} $NaClO_4$, both 0.2 mol dm^{-3} in Tris buffer at the appropriate pH. After 5–20 min at 25 °C the solution was quenched to pH ~3 with dilute hydrochloric acid, diluted with water, and sorbed on and then eluted from SP-C25 cation-exchange resin with 0.25 mol dm^{-3} NaCl (for $[Co(en)_2(\beta\text{-alaO})]^{2+}$) and then 0.5 mol dm^{-3} NaCl (for $[Co(en)_2(OH_2)(\beta\text{-alaO-}i\text{-Pr})]^{3+}$). Absorbances at 490 nm were measured and amounts evaluated by using ϵ_{490} values of 128 and 77, respectively.

^{18}O enrichments were determined as previously described.[1] Enriched water was purchased from Bio-Rad (~1 atom % ^{18}O) or Alfa Products (~10 atom % ^{18}O) and incorporated into the complex as coordinated H_2O by carrying out the preparation of *cis*-$[Co(en)_2(OH_2)(\beta\text{-alaO-}i\text{-Pr})](NO_3)_2(ClO_4)$ in the enriched solvent and into $[Co(en)_2(\beta\text{-alaO-}i\text{-Pr})](ClO_4)_3$ by preparing and using carbonyl-^{18}O-labeled β-alanine isopropyl ester. β-alanine–hydrochloride (10.0 g) in enriched H_2O (10 cm^3, 2.8 atom % ^{18}O) containing concentrated hydrochloric acid (0.5 cm^3) was refluxed under N_2 for 24 h, reduced to half-volume by rotary evaporation, and crystallized by pouring into stirred dry acetone (200 cm^3). The product was washed with Et_2O and dried over P_2O_5. This material (8.3 g) was dissolved in 100 cm^3 of cold dry 2-propanol to which $SOCl_2$ (10 cm^3) had been added. After 3-h reflux the volume was reduced to ca. 50 cm^3 and Et_2O (300 cm^3) slowly added with stirring. The crystalline β-alaO-*i*-Pr·HCl was collected, washed with Et_2O, and dried over P_2O_5. The ^{18}O content of aqueous solutions (~1 cm^3) was determined by equilibration with normal CO_2 (ca. 0.05 mmol) at 80 °C.[1]

Coordinated water in *cis*-$[Co(en)_2(^{18}OH_2)(\beta\text{-alaO-}i\text{-Pr})](NO_3)_2(ClO_4)$ (0.4 g) was removed by heating the anhydrous complex at 80 °C for 2 h on a vacuum line. ^{18}O in $[Co(en)_2(\beta\text{-alaO-}i\text{-Pr})](ClO_4)_3$ was determined by hydrolyzing a sample (0.3 g) in water at pH 9.0, collecting $[Co(en)_2(\beta\text{-alaO})](HgI_4)$, and pyrolyzing it as described previously[6] to recover β-alanine. Aqueous samples of $[Co(en)_2(\beta\text{-alaO})]^{2+}$ were ana-

(4) This is now known to be incorrect, but details of the HOCl reaction remain obscure.
(5) Buckingham, D. A.; Foster, D. M.; Sargeson, A. M. *J. Am. Chem. Soc.* **1969**, *91*, 4102.
(6) Baraniak, E.; Buckingham, D. A.; Clark, C. R.; Sargeson, A. M., submitted for publication in *Inorg. Chem.*
(7) Baraniak, E.; Buckingham, D. A.; Clark, C. R.; Sargeson, A. M., submitted for publication in *Inorg. Chem.*

lyzed similarly following precipitation as $[Co(en)_2(\beta\text{-alaO})](HgI_4)$.

β-alaO-*i*-Pr·HCl was recovered from *cis*-$[Co(en)_2(OH_2)(\beta\text{-alaO-}i\text{-Pr})]^{3+}$ produced from $[Co(en)_2(\beta\text{-alaO-}i\text{-Pr})](ClO_4)_3$ as follows. Carbonyl-^{18}O-labeled $[Co(en)_2(\beta\text{-alaO-}i\text{-Pr})](ClO_4)_3$ (1.5 g) was dissolved in 30 cm^3 of 1.0 mol dm^{-3} $NaHCO_3$ solution at pH 8.1. After 5 min 30 cm^3 of 1.0 mol dm^{-3} $HClO_4$ was added and the diluted solution (ca. 1 dm^3) sorbed on SP-C25 cation-exchange resin. NaCl solution 0.2 mol dm^{-3} was used to separate and elute $[Co(en)_2(\beta\text{-alaO})]^{2+}$ from *cis*-$[Co(en)_2(OH_2)(\beta\text{-alaO-}i\text{-Pr})]^{3+}$, which was finally removed with 0.5 mol dm^{-3} NaCl. $[Co(en)_2(\beta\text{-alaO})]^{2+}$ was precipitated as the HgI_4^{2-} salt following concentration of the eluate to ca. 100 cm^3. The 3+ monodentate ester complex was also reduced in volume (80 cm^3) and electrolyzed at −1.2 V (SCE) until the current was less than 2 μA (2 h) with maintenance of the pH at ca. 4 by dropwise addition of HCl. The Co(II) solution was taken to dryness and extracted with acetone (four times); the dried residue was reextracted with dry acetone and Co(II) removed from the residue by addition of $Na_2C_2O_4$ (0.3 g) to an aqueous solution (2 cm^3). The residue was taken again to dryness and chromatographed on silica with 4% aqueous acetone and the ester band collected and converted to the Cl^- salt on a short column of AG1X4 anion-exchange resin. The β-alaO-*i*-Pr·HCl product was recrystallized from acetone by adding Et_2O containing a drop of $SOCl_2$ (recovered 40 mg).

The following experiments were carried out using *cis*-$[Co(en)_2(^{18}OH_2)(\beta\text{-alaO-}i\text{-Pr})](NO_3)_3$.

(1) Acid Hydrolysis. The complex (1.8 g) dissolved in 1 mol dm^{-3} HCl (25 cm^3) was maintained at 25.0 °C for 17 h and then sorbed on and eluted from cation-exchange resin. $[Co(en)_2(\beta\text{-alaO})]^{2+}$ was separated with 1 mol dm^{-3} NaCl, reduced in volume, and precipitated as the HgI_4^{2-} salt, and β-alanine was recovered as detailed above. Unreacted *cis*-$[Co(en)_2(OH_2)(\beta\text{-alaO-}i\text{-Pr})]^{3+}$ sorbed to the resin was neutralized to pH 7, washed with water, and then made basic to pH ~13 (5 min) before again quenching to pH 4. Elution with 1 mol dm^{-3} $NaClO_4$ led to the recovery of $[Co(en)_2(\beta\text{-alaO})]^{2+}$, which was analyzed as before.

(2) Alkaline Hydrolysis. To the complex (1.1 g) dissolved in 1 mol dm^{-3} $NaClO_4$ (25 cm^3) was added 25 cm^3 of 1.0 mol dm^{-3} NaOH and the solution maintained at 25.0 °C for 10 min. Following quenching to pH ~4 (HOAc) and dilution, the products were sorbed on and then eluted from cation-exchange resin (Na^+ form), first at pH ~9 (to remove 1+ ions) and then under neutral conditions (2 mol dm^{-3} $NaClO_4$). The $[Co(en)_2(\beta\text{-alaO})]^{2+}$ product was collected and treated as above.

Results

Chelated Ester. Unlike the chelated glycine esters, which hydrolyze rapidly in aqueous acid (R = Me, $t_{1/2}$ = 26 s; R = *i*-Pr, $t_{1/2}$ = 10 min)[8] and even more rapidly in alkali,[2] $[Co(en)_2(\beta\text{-alaOR})](ClO_4)_3$ is kinetically more stable. Thus the R = *i*-Pr complex has been characterized following recrystallization from acidified warm water. The complexes are reasonably stable as solids, but some decomposition had occurred with R = Me after 5 years.

Ester hydrolysis does however occur in aqueous solutions, and it does so with retention of the chelate ring. $[Co(en)_2(\beta\text{-alaO})]^{2+}$ is the only product under most conditions. Possible $[Co(en)_2(OH_2/OH)(\beta\text{-alaO/R})]^{3+/2+/+}$ products containing the monodentate ester or acid functions are not formed in measurable amounts (<2%). Figure 1A gives the ^{1}H NMR spectrum of $[Co(en)_2(\beta\text{-alaO-}i\text{-Pr})]^{3+}$ in 0.1 mol dm^{-3} DCl and Figure 1C its hydrolysis products after 36 h at ~25 °C. No monodentate ester complex, $[Co(en)_2(OD_2)(\beta\text{-alaO-}i\text{-Pr})]^{3+}$, is formed during this time; since *cis*-$[Co(en)_2(OD_2)(\beta\text{-alaO-}i\text{-Pr})]^{3+}$ reacts more slowly (see below), it would have appeared in the NMR spectrum had it been formed (Figure 1B). A similar conclusion holds for the possible $[Co(en)_2(OH_2)(\beta\text{-alaO})]^{2+}$ + *i*-PrOH products. The inset to the figure shows the relative positions of the methyl doublet of the isopropyl group in the three situations. Following alkaline hydrolysis ion-exchange analysis gave a more accurate estimate since $[Co(en)_2(OH)(\beta\text{-alaO/R})]^{+,2+}$ can easily be separated from $[Co(en)_2(\beta\text{-alaO})]^{2+}$ by acidic eluants. A distinction between $[Co(en)_2(\beta\text{-alaO})]^{2+}$ + *i*-PrOH, $[Co(en)_2(OH)(\beta\text{-alaO})]^+$ + *i*-PrOH, and $[Co(en)_2(OH)(\beta\text{-alaO-}i\text{-Pr})]^{2+}$ cannot be made with certainty by the NMR method in alkaline solution, but it can easily be made by ion-exchange chromatography.

Some buffers catalyze hydrolysis while others result in substituted products. Most amines add directly to form the chelated amide $[Co(en)_2(\beta\text{-alaNR}_1R_2)]^{3+}$, which can easily be distinguished and isolated. This reaction is considered in detail in the following publication.[9] Similarly, HCO_3^-/CO_3^{2-} buffers result in some $[Co(en)_2(OCO_2)(\beta\text{-alaO-}i\text{-Pr})]^+$ (see below). However, imidazole and *N*-methylimidazole give only $[Co(en)_2(\beta\text{-alaO})]^{2+}$, as does HPO_4^{2-}. Conventional nonnucleophilic buffers (Hepes, Tris, lutidine, morpholine, NEt_3) do not catalyze hydrolysis. For these the stoichiometries given by eq 5 and 6 hold. $(+)_{589}$-$[Co(en)_2(\beta\text{-alaO-}i\text{-Pr})]^{3+}$ + H_2O → $[Co(en)_2(\beta\text{-alaO})]^{2+}$ + HO-*i*-Pr + H^+ (5)

$[Co(en)_2(\beta\text{-alaO-}i\text{-Pr})]^{3+}$ + OH^- → $[Co(en)_2(\beta\text{-ala})]^{2+}$ + HO-*i*-Pr (6)

$(\beta\text{-alaO-}i\text{-Pr})]^{3+}$ prepared from $(+)_{589}$-$[Co(en)_2Br(\beta\text{-alaO-}i\text{-Pr})]^{2+}$ when treated with 3 mol dm^{-3} HCl and at pH 10.6 (0.1 mol dm^{-3} NEt_3 buffer) gave optically pure $(+)_{589}$-$[Co(en)_2(\beta\text{-alaO})]^{2+}$ ($[M]_{589}$ = 900° mol^{-1} dm^3 m^{-1}) following ion-exchange workup.

Rate data were obtained spectrophotometrically. Figure 2 gives spectral changes occurring during hydrolysis under acidic conditions, and rate data collected at 495 nm gave excellent linear log $(A_\infty - A_t)$ vs. time plots. Table I lists k_{obsd} values that show an independence in $[H^+]$ over the pH range 0–4. No HOAc or OAc^- catalysis was observed. Data in D_2O give k_{H_2O/D_2O} = 2.5 for R = *i*-Pr. The methyl ester chelate hydrolyzes some 12 times faster than the isopropyl ester. Table II (supplementary data) gives rate data in alkaline solution. This is summarized by Figure 3. Buffered solutions were used, and the data represent k_{obsd} at $[Buffer]_T$ = 0. No measurable catalysis was found with 2,6-lutidine (0–1.0 mol dm^{-3}), Tris (0–0.50), morpholine (0–0.50), and Et_3N (0–0.50) buffers. Three regions of reactivity are ap-

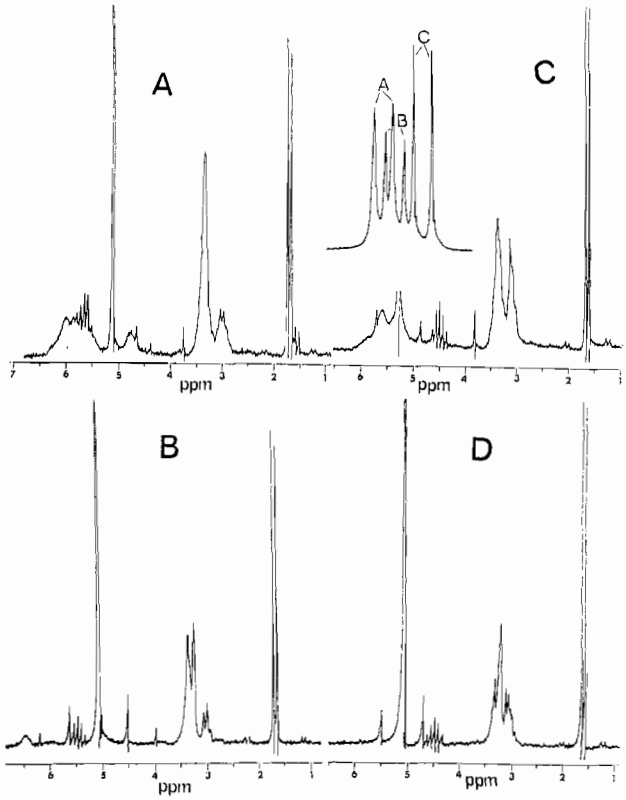

Figure 1. ^{1}H NMR spectra (90 MHz) of (A) $[Co(en)_2(\beta\text{-alaO-}i\text{-Pr})]^{3+}$ in 0.01 mol dm^{-3} DCl, (C) the solution in part A after 36 h, giving $[Co(en)_2(\beta\text{-alaO})]^{2+}$ + *i*-PrOD hydrolysis products, (B) *cis*-$[Co(en)_2(H_2O)(\beta\text{-alaO-}i\text{-Pr})]^{3+}$ in D_2O, and (D) the solution in part B after 3 days at pD ~9, giving $[Co(en)_2(\beta\text{-alaO})]^{2+}$ + *i*-PrOD hydrolysis products. The inset distinguishes the methyl doublets of the isopropyl group in (A) 1.76 ppm, (B) 1.71 ppm, and (C, D) 1.61 ppm.

(8) Alexander, M. D.; Busch, D. H. *J. Am. Chem. Soc.* **1966**, *88*, 1130.

(9) Buckingham, D. A.; Clark, C. R. *Inorg. Chem.*, following paper in this issue.

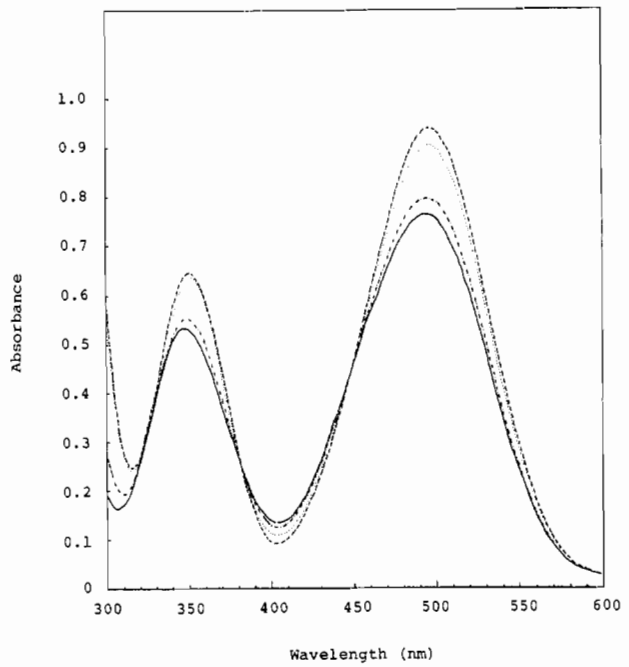

Figure 2. Spectral changes during hydrolysis of $[Co(en)_2(\beta\text{-alaO-}i\text{-Pr})]^{3+}$ to $[Co(en)_2(\beta\text{-alaO})]^{2+}$ in 0.10 mol dm^{-3} $HClO_4$: — (t = 0), -·- (1.5 h), ··· (16 h), - - - (36 h).

Table I. Rate Data for Hydrolysis of $[Co(en)_2(\beta\text{-alaOR})]^{3+}$ in Acid Solution (25.0 °C, I = 1.0 ($NaClO_4$))[a]

R	$[HClO_4]$, mol dm^{-3}	$10^5 k_{obsd}$, s^{-1}	$10^6 k_{H_2O}$,[b] mol^{-1} dm^3 s^{-1}
Me	1.00	55	9.9
	0.01	53	9.5
i-Pr	1.00	4.6	0.83
	0.10	4.7	0.85
	0.01	4.6	0.83
	0.01[c]	1.86	0.37
	d	4.7	0.85
	e	4.7	0.85

[a] [Co] = 4 × 10^{-4}–2 × 10^{-2} mol dm^{-3}, λ = 495 nm. [b] $k_{H_2O} = k_{obsd}/55.5$, $k_{D_2O} = k_{obsd}/50$. [c] D_2O solution. [d] 0.2 mol dm^{-3} HOAc/OAc$^-$ buffer, pH 4.46. [e] 0.1 mol dm^{-3} HOAc/OAc$^-$ buffer, pH 4.48.

parent in Figure 3. For pH 6.2–7.5 and for pH >10 the rate is first order in $[OH^-]$, from pH 7.5 to 10 the rate approaches second-order kinetics in $[OH^-]$. Overall the data fit expression 7, with k^I = 5.0 × 10^3 mol^{-1} dm^3 s^{-1}, k^{II} = 7.0 × 10^8 mol^{-2} dm^6

$$k_{obsd} = \frac{k^I[OH^-] + k^{II}[OH^-]^2}{1 + K[OH^-]} \quad (7)$$

s^{-1}, K = 1.75 × 10^4 mol^{-1} dm^3, at 25.0 °C and I = 1.0. Data in D_2O (Figure 3) gives k^I = 5.6 × 10^3 mol^{-1} dm^3 s^{-1}, k^{II} = 9.45 × 10^8 mol^{-2} dm^6 s^{-1}, whence kinetic isotope ratios of 0.89 and 0.74 obtain in the two extreme first-order regions. Activation enthalpy ($\Delta H^\ddagger$ = 25.4 kJ mol^{-1}) and entropy ($\Delta S^\ddagger$ = −72 J mol^{-1} K^{-1}) parameters were obtained from the data: 7.85 s^{-1} (10 °C, pH 10.86, pK_w = 14.32), 14.8 s^{-1} (20.0, 10.58, 13.94), and 24.1 s^{-1} (33.0, 10.29, 13.60).

Significant buffer catalysis occurred with HPO_4^{2-} (pK_a = 6.5) and HCO_3^- (6.0) (see below) and measurable catalysis with imidazole (7.27), *N*-methylimidazole (7.40), and glycine ethyl ester (7.82). Kinetic data (Table III, supplementary data) show the basic form to be the catalyzing species, and Table IV lists k_B values. It is clear that k_B is unrelated to the pK_a of the buffer. No measurable catalysis occurred with PO_4^{3-} or CO_3^{2-}. In D_2O solutions the k_B value for DPO_4^{2-} gives $k_{HPO_4^{2-}}/k_{DPO_4^{2-}}$ = 2.04.

Table V gives ^{18}O tracer results. Experiments 1–3 detail incorporation of tracer into the carbonyl function of *cis*-$[Co(en)_2Br(\beta\text{-alaO-}i\text{-Pr})]^{2+}$, which was then converted to the chelated ester $[Co(en)_2(\beta\text{-alaO-}i\text{-Pr})](NO_3)_3$ (not analyzed). Hydrolysis

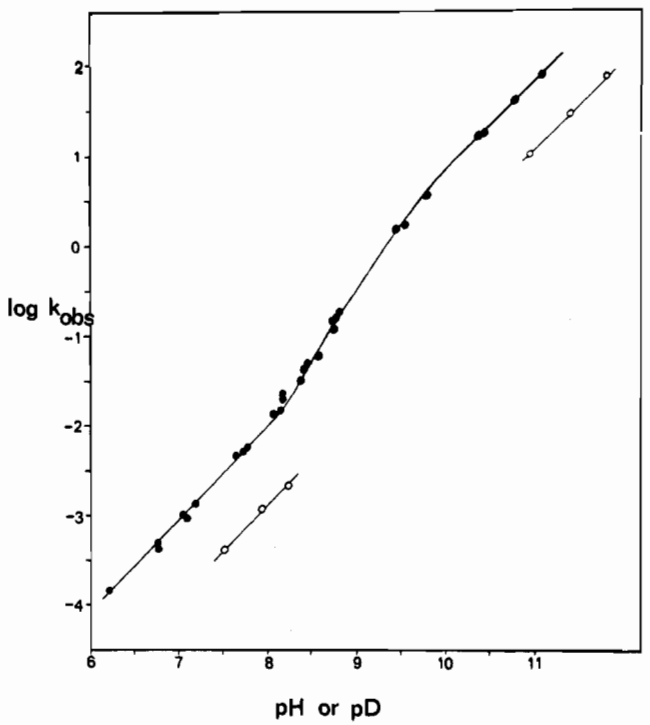

Figure 3. log k_{obsd} (extrapolated to $[Buffer]_T$ = 0.0 mol dm^{-3}) vs. pH (closed circles) or pD (open circles) rate profile for the alkaline hydrolysis of $[Co(en)_2(\beta\text{-alaO-}i\text{-Pr})]^{3+}$ to give $[Co(en)_2(\beta\text{-alaO})]^{2+}$ (I = 1.0 ($NaClO_4$), 25.0 °C).

Table IV. k_B Values for Buffer-Catalyzed Hydrolysis of $[Co(en)_2(\beta\text{-alaO-}i\text{-Pr})]^{3+}$ (25.0 °C, I = 1.0 ($NaClO_4$))

buffer species (pK_a)	pH range	$[B]_T$ range, mol dm^{-3}	$10^3 k_B$ mol^{-1} dm^3 s^{-1}
HPO_4^{2-} (6.5)	5.77–6.98	0–0.500	30
DPO_4^{2-} (6.88)[a]	6.85, 7.02	0.125, 0.250	14.7
HCO_3^- (3.9)	8.22, 7.97	0–0.93	40
imidazole (7.27)	6.86–7.77	0–0.5	8
imidazole[9]	7.32–8.28	0–1.0	4.5
N-methylimidazole (7.40)	6.93–7.88	0–1.0	6
glyOEt (7.82)[9]	7.32–8.28	0–1.0	3.0

[a] pD or pK_a (D_2O) values from pD = pH + 0.4.

at pH 9 results in 96% retention of label in the $[Co(en)_2(\beta\text{-alaO})]^{2+}$ product (experiment 4), and experiment 5 shows that this essentially remains in 1 mol dm^{-3} $HClO_4$ after 20 days. Under such conditions the similarly labeled $[Co(en)_2(glyO)]^{2+}$ chelate (VI) shows little exchange, whereas when the label is introduced

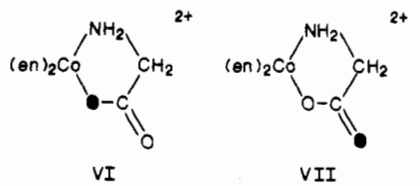

VI VII

into the exo position (VII), the half-time for exchange is about 8 days.[1] The labeled oxygen in $[Co(en)_2(\beta\text{-alaO-}i\text{-Pr})]^{3+}$ is therefore coordinated to the metal and remains in this position on hydrolysis ro $[Co(en)_2(\beta\text{-alaO})]^{2+}$.

Monodentate Ester. In a separate publication we have shown that the Hg^{2+}-induced hydrolysis of *cis*-$[Co(en)_2X(\beta\text{-alaO-}i\text{-Pr})]^{2+}$ (X = Cl, Br) results in some 90% *cis*-$[Co(en)_2(OH_2)(\beta\text{-alaO-}i\text{-Pr})]^{3+}$ with the remainder being the chelated ester.[7] Recrystallization of this material from aqueous ethanol in the presence of $LiNO_3$ and $LiClO_4$ results in the recovery of *cis*-$[Co(en)_2(OH_2)(\beta\text{-alaO-}i\text{-Pr})](NO_3)_2(ClO_4)$. The uncoordinated ester function shows a strong carbonyl absorption at 1725 cm^{-1} (similar to that of the free ligand hydrochloride salt), and the ^1H NMR spectra of both the aqua and hydroxo complexes (Figure 1B giving

Table V. ^{18}O Tracer Results

expt	conditions	compd/complex analyzed	R_{46}	% ^{18}O[a]
1		β-alaOH·HCl	0.041160	2.046
2		β-alaO-*i*-Pr·HCl	0.017662	0.888
3		*cis*-$[Co(en)_2Br(\beta\text{-alaO-}i\text{-Pr})]Br_2$	0.016835	0.847
4	$[Co(en)_2(\beta\text{-alaO-}i\text{-Pr})]^{3+}$; pH 9, 2 h	$[Co(en)_2(\beta\text{-alaO})](HgI_4)$	0.016330	0.822
5	$[Co(en)_2(\beta\text{-alaO})]^{2+}$; 20 days, 1 mol dm^{-3} $HClO_4$	$[Co(en)_2(\beta\text{-alaO})](HgI_4)$	0.016181	0.815
6	$[Co(en)_2(\beta\text{-alaO-}i\text{-Pr})]^{3+}$; 1 mol dm^{-3} HCO_3^-, pH 8.1, 5 min	β-alaO-*i*-PrHCl from *cis*-$[Co(en)_2(OH)(\beta\text{-alaO-}i\text{-Pr})]^{2+}$	0.004120	0.208
7	as in expt 6	$[Co(en)_2(\beta\text{-alaO})](HgI_4)$	0.015892	0.800
8		H_2O	0.025220	1.264
9		*cis*-$[Co(en)_2(^{18}OH_2)(\beta\text{-alaO-}i\text{-Pr})](NO_3)_3$	0.021589	1.084
10	$[Co(en)_2(^{18}OH_2)(\beta\text{-alaO-}i\text{-Pr})]^{3+}$; 0.1 mol dm^{-3} NEt_3, pH 11.10, 2.5 h	$[Co(en)_2(\beta\text{-alaO})](HgI_4)$	0.012170	0.614
11	$[Co(en)_2(^{18}OH_2)(\beta\text{-alaO-}i\text{-Pr})]^{3+}$; 1 mol dm^{-3} HCl, 17 h	$[Co(en)_2(\beta\text{-alaO})](HgI_4)$	0.010198	0.515
12	as in expt 11, recovered; 0.1 mol dm^{-3} NaOH, 10 min	$[Co(en)_2(^{18}OH_2)(\beta\text{-alaO-}i\text{-Pr})]^{3+}$	0.008190	0.414

[a] % $^{18}O = 100R/(1.97 + R)$; % ^{18}O in CO_2 (normal abundance) = 0.201.

Table VI. Rate Data for Hydrolysis of *cis*-$[Co(en)_2(OH_2)(\beta\text{-alaO-}i\text{-Pr})]^{3+}$ in Acid Solution (25.0 °C, I = 1.0 ($NaClO_4$))[a]

$[HClO_4]$, mol dm^{-3}	10^6k_{obsd}, s^{-1}	$[HClO_4]$, mol dm^{-3}	10^6k_{obsd}, s^{-1}
1.00	1.8	0.01	1.8
1.00	2.0[b]	0.01	1.8[b]
0.50	1.8	1.00	1.8[c]
0.10	1.8		

[a] [Co] = 4 × 10^{-4}–4 × 10^{-3} mol dm^{-3}; λ = 495 nm, spectrophotometric data. [b] Ion-exchange data. [c] 1.0 mol dm^{-3} $DClO_4$ solution.

that of the hydroxo complex) give the *gem*-methyl doublet at 1.71 ppm, intermediate between that for the chelate and *i*-PrOH. Spectrophotometric and pH-stat titrations give $pK_a = 6.05 \pm 0.05$ for the coordinated aqua ligand (25.0 °C, I = 1.0 ($NaClO_4$); eq 8). Visible spectra for the 3+ aqua and 2+ hydroxo complexes

$$cis\text{-}[Co(en)_2(OH_2)(\beta\text{-alaO-}i\text{-Pr})]^{3+} + H_2O \overset{K_a}{\rightleftharpoons} cis\text{-}[Co(en)_2(OH)(\beta\text{-alaO-}i\text{-Pr})]^{2+} + H_3O^+ \quad (8)$$

are less intense (ϵ_{489} 77 ± 2 for *cis*-$[Co(en)_2(OH_2)(\beta\text{-alaO-}i\text{-Pr})]^{3+}$, ϵ_{500} 100 ± 2 for *cis*-$[Co(en)_2(OH)(\beta\text{-alaO-}i\text{-Pr})]^{2+}$) than that for the hydrolyzed chelate $[Co(en)_2(\beta\text{-alaO})]^{2+}$ (ϵ_{195} 128)[7] but are of similar intensity to that for the ester chelate (ϵ_{493} 98).

Ester hydrolysis in $[Co(en)_2(OH_2)(\beta\text{-alaO-}i\text{-Pr})]^{3+}$ is considerably slower than for the chelate. Isosbestic points are maintained in the visible spectrum (0.1 mol dm^{-3} $HClO_4$), and ion-exchange of the product shows it is entirely the 2+ ion $[Co(en)_2(\beta\text{-alaO})]^{2+}$; i.e., chelation has occurred on hydrolysis. *cis*- and *trans*-$[Co(en)_2(OH_2)(\beta\text{-alaO})]^{2+}$ [6] can be distinguished from $[Co(en)_2(\beta\text{-alaO})]^{2+}$ by elution at pH ~8 when they move as 1+ ions. Equation 9 therefore holds under acidic conditions. Spectro-

$$cis\text{-}[Co(en)_2(OH_2)(\beta\text{-alaO-}i\text{-Pr})]^{3+} \rightarrow [Co(en)_2(\beta\text{-alaO})]^{2+} + i\text{-PrOH} + H^+ \quad (9)$$

photometric rate data (Table VI) give $k_0 = 1.8 \times 10^{-6}$ s^{-1} from 1.0 to 0.01 mol dm^{-3} $HClO_4$. The same rate was observed in D_2O.

In alkaline solution a two-term rate expression holds (eq 10). The data (Table VII, supplementary data) were obtained under pH-stat control, in buffers, or at high pH with NaOH solutions.

$$k_{obsd} = k_0 + k_{OH}[OH^-] \quad (10)$$

In buffers, the data correspond to k_{obsd} at $[Buffer]_T = 0$. Figure 4 summarizes k_{obsd} as a function of pH giving $k_0 = (5.6 \pm 0.5) \times 10^{-6}$ s^{-1} and $k_{OH} = 0.22 \pm 0.02$ mol^{-1} dm^3 s^{-1} at 25.0 °C and I = 1.0 mol dm^{-3}. Figure 1D gives the ^1H NMR spectrum following hydrolysis of *cis*-$[Co(en)_2(OH)(\beta\text{-alaO-}i\text{-Pr})]^{2+}$ at pD ~10, but this does not distinguish between retention of the monodentate function with formation of $[Co(en)_2(OH)(\beta\text{-alaO})]^+$ + *i*-PrOH and chelation and hydrolysis to give $[Co(en)_2(\beta\text{-alaO})]^{2+}$ + *i*-PrOH. However, ion-exchange analysis allows this distinction. For the pH-stat-controlled experiments and in non-catalyzing buffers (e.g. NEt_3) and NaOH solution, three products result, $[Co(en)_2(\beta\text{-alaO})]^{2+}$ (60 ± 5%), *cis*-$[Co(en)_2(OH)(\beta\text{-alaO})]^+$ (33 ± 5%), and *trans*-$[Co(en)_2(OH)(\beta\text{-alaO})]^+$ (7 ± 4%). Table VIII gives these results. Their approximate constancy over the pH range 10.4–13.5 requires that each follows a first-order $[OH^-]$ dependence. The *cis*- and *trans*-$[Co(en)_2(OH)(\beta\text{-alaO})]^+$ ions separate from each other as mauve and red bands, respectively, at pH ~8 on a long ion-exchange column, and they elute well before the orange $[Co(en)_2(\beta\text{-alaO})]^{2+}$ ion. Table IX gives spectral details used in this analysis. Above pH 12.5 (NaOH solutions) the increased yields of the trans 1+ ion may result from contamination by *trans*-$[Co(en)_2(OH)_2]^+$ since the two coelute, and it is known that $[Co(en)_2(\beta\text{-alaO})]^{2+}$ and *cis*-$[Co(en)_2$-

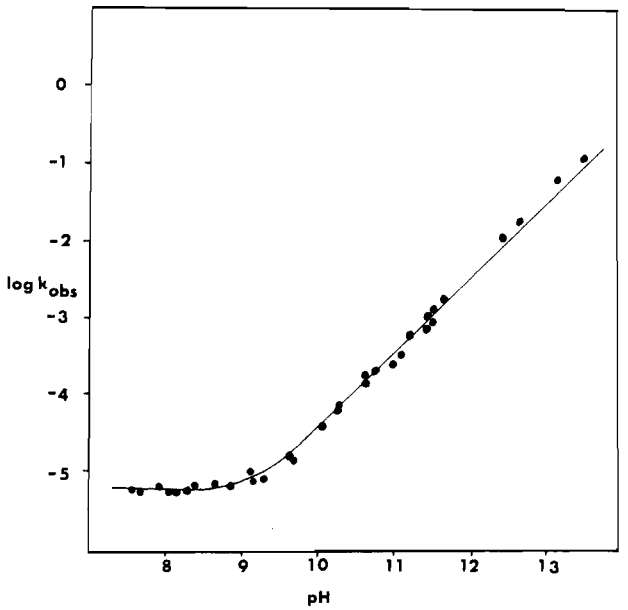

Figure 4. log k_{obsd} (extrapolated to $[Buffer]_T = 0.0$ mol dm^{-3}) vs. pH rate profile for the cyclization and hydrolysis of *cis*-$[Co(en)_2(OH)(\beta\text{-alaO-}i\text{-Pr})]^{2+}$ in alkaline solution (I = 1.0 ($NaClO_4$), 25.0 °C).

Table VIII. Product of the Alkaline Hydrolysis of *cis*-$[Co(en)_2(OH)(\beta\text{-alaO-}i\text{-Pr})]^{2+}$ (25.0 °C, I = 1.0 ($NaClO_4$))[a]

pH	% *trans*-$[Co(en)_2(OH)(\beta\text{-alaO})]^+$	% *cis*-$[Co(en)_2(OH)(\beta\text{-alaO})]^+$	% $[Co(en)_2(\beta\text{-alaO})]^{2+}$
13.5[b]	16	32	51
12.8[b]	18	34	48
12.5	16	33	50
11.9	11	38	51
11.7	8	34	58
11.6	10	32	55
11.5	11	32	58
10.8	8	31	61
10.6	6	34	60
10.4	8	31	61

[a] Analysis following hydrolysis of ca. 0.1 g of $[Co(en)_2(OH_2)(\beta\text{-alaO-}i\text{-Pr})](NO_3)_2(ClO_4)$; averages for three experiments with quenching after $10t_{1/2}$. [b] Hand-mixed with a 10-fold excess of NaOH.

Table IX. Spectral Properties of Products of Alkaline Hydrolysis of *cis*-$[Co(en)_2(OH)(\beta\text{-alaO-}i\text{-Pr})]^{2+}$ [a]

complex	λ_{max}, nm	ϵ_{max}
trans-$[Co(en)_2(OH)(\beta\text{-alaO})]^+$	500	76
	360	
cis-$[Co(en)_2(OH)(\beta\text{-alaO})]^+$	500	91
	360	
$[Co(en)_2(\beta\text{-alaO})]^{2+}$	495	128
	350	90
trans-$[Co(en)_2(OH_2)(\beta\text{-alaOH})]^{3+}$ [b]	495	55
	350	60
cis-$[Co(en)_2(OH_2)(\beta\text{-alaOH})]^{3+}$ [b]	490	72
	350	65

[a] Solutions in 0.4–2.0 mol dm^{-3} $NaClO_4$, pH 8–9. [b] Solutions on acidification to pH ca. 2; estimations of amounts formed carried out under this condition.

Table X. OH^- Consumption[a] for the Hydrolysis of *cis*-$[Co(en)_2(OH_2)(\beta\text{-alaO-}i\text{-Pr})]^{3+}$ (25.0 °C, I = 1.0 ($NaClO_4$))

pH	% $[Co(en)_2(\beta\text{-alaO})]^{2+}$ [b]	equiv of OH^- consumed/equiv of complex: obsd	calcd[c]
11.7	0.58	1.43	1.42
11.3	0.58	1.35	1.42
10.4	0.62	1.34	1.38

[a] pH-stat control; 0.2–0.5 g of $[Co(en)_2(OH_2)(\beta\text{-alaO-}i\text{-Pr})](NO_3)_2(ClO_4)$. [b] Spectrophotometric analysis following ion-exchange separation. [c] 1 equiv of OH^- is immediately consumed on neutralization of coordinated water, and the remainder is slowly consumed as $[Co(en)_2(OH)(\beta\text{-alaO})]^+$ is formed.

$(OH)(\beta\text{-alaO})]^+$ slowly form *trans*-$[Co(en)_2(OH)_2]^+$ at high pH.[6] The stoichiometry of eq 11 requires 1 equiv of OH^- to be consumed for that part of the reaction leading to $[Co(en)_2(OH)(\beta\text{-alaO})]^+$, and the pH-stat data given in Table X substantiate this consumption.

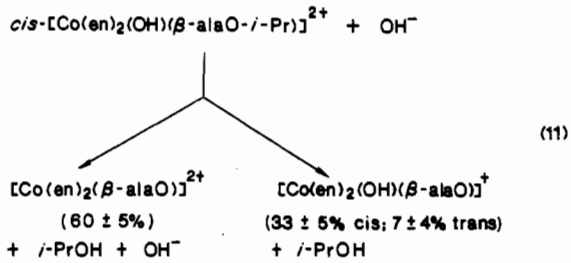

(11)

Experiments carried out with optically pure $(+)_{589}$-$[Co(en)_2(OH_2)(\beta\text{-alaO-}i\text{-Pr})]^{3+}$ generated from $(+)_{589}$-$[Co(en)_2Br(\beta\text{-alaO-}i\text{-Pr})]^{2+}$ [7] show that both acid and alkaline hydrolyses result in full retention of configuration about the metal (Table XI). The reactant contained some 10% $(+)_{589}$-$[Co(en)_2(\beta\text{-alaO-}i\text{-Pr})]^{3+}$ (produced in the synthesis[7]), but this also hydrolyzes under both sets of conditions with full retention of configuration (see above). The product produced from $(+)_{589}$-$[Co(en)_2(OH_2)(\beta\text{-alaO-}i\text{-Pr})]^{3+}$ in acid solution was analyzed in 3 mol dm^{-3} HCl as well as after elution from ion-exchange resin using 2 mol dm^{-3} $NaClO_4$. The separate *cis*-$[Co(en)_2(OH)(\beta\text{-alaO})]^+$ and $[Co(en)_2(\beta\text{-alaO})]^{2+}$ ions produced at pH 10.62 in NEt_3 buffer both show full retention of chirality. The former ion was analyzed following its cyclization to $[Co(en)_2(\beta\text{-alaO})]^{2+}$ in acid solution; this reaction is slow but also quantitative.[10] As expected, the small amount of *trans*-$[Co(en)_2(OH)(\beta\text{-alaO})]^+$ produced showed no rotation. It is not clear how this species arises.

Buffer catalysis in alkaline solution usually results in $[Co(en)_2(\beta\text{-alaO})]^{2+}$. This was clearly demonstrated for PO_4^{3-} and CO_3^{2-}, but the small contributions to the rate by the other buffers mean that this aspect remains uncertain for them. Table XII (supplementary data) gives rate data, and Table XIII summarizes these as a list of k_B values. The full rate law takes the form of eq 12. It is significant that PO_4^{3-} and CO_3^{2-} have by far the

$$k_{obsd} = k_0 + k_{OH}[OH^-] + k_B[B] \qquad (12)$$

largest k_B values and that HPO_4^{2-} and HCO_3^- are not effective. However, when *cis*-$[Co(en)_2(OH)(\beta\text{-alaO-}i\text{-Pr})]^{2+}$ was treated at pH 7.90 with 1.0 mol dm^{-3} glycine ethyl ester (two experiments) and 0.5 mol dm^{-3} glycine ethyl ester (one experiment), 28%, 30%, and 15% respectively, of $[Co(en)_2(\beta\text{-ala-glyOEt})]^3$ was recovered. Furthermore, the presence of the glycine ester did not measurably affect the rate. These experiments suggest formation of the chelated ester as an intermediate under these conditions.

Experiments 8 and 9 of Table V show the fate of the ^{18}O label of the coordinated water ligand in the cyclization of *cis*-$[Co(en)_2(^{18}OH_2)(\beta\text{-alaO-}i\text{-Pr})]^{3+}$. Alkaline hydrolysis at pH 11.10 (NEt_3 buffer) results in almost complete retention of label (94%), which must now be incorporated into the β-alanine chelate (experiment 10). In 1.0 mol dm^{-3} HCl chelation is much slower (k_{obsd} = 1.8 × 10^{-6} s^{-1}, see above), and after 17 h only some 10% of $[Co(en)_2(\beta\text{-alaO})]^{2+}$ was recovered from the ion-exchange column. However, this product retains 71% of the O label (experiment 11), which again must be incorporated into the chelate. The remaining unreacted *cis*-$[Co(en)_2(OH_2)(\beta\text{-alaO-}i\text{-Pr})]^{3+}$ ion was recovered and treated with 0.1 mol dm^{-3} NaOH (pH ~12) for 10 min. The recovered $[Co(en)_2(\beta\text{-alaO})]^{2+}$ ion retained 48% of the original enrichment (experiment 12).

Chelated Ester + HCO_3^-. This most unusual reaction, unique in our experience, was first noticed in ^1H NMR experiments. Figure 5 shows the isopropyl doublet of the ester on adding HCO_3^- to buffered and self-buffered solutions of $[Co(en)_2(\beta\text{-alaO-}i\text{-Pr})]^{3+}$ in D_2O. The growth of the 1.71-ppm doublet between that for $[Co(en)_2(\beta\text{-alaO-}i\text{-Pr})]^{3+}$ at 1.76 ppm and that for *i*-PrOH at 1.62 ppm demonstrates the presence of an intermediate species that slowly decays to *i*-PrOH. Positive identification as $[Co(en)_2(OCO_2)(\beta\text{-alaO-}i\text{-Pr})]^+$ was provided by spiking the reaction mixture with authentic $[Co(en)_2(OH_2)(\beta\text{-alaO-}i\text{-Pr})]^{3+}$ under the same conditions. If this product is chromatographed at pH ~8 on Na^+ form Dowex, a rapidly moving mauve 1+ band separates (considerable streaking from orange $[Co(en)_2(\beta\text{-alaO})]^{2+}$, but if acid quenching precedes chromatography under neutral conditions, the product is strongly retained as the orange $[Co(en)_2(OH_2)(\beta\text{-alaO-}i\text{-Pr})]^{3+}$ ion. Positive identification of the latter was provided by visible spectra under acidic and alkaline conditions and by the recovery of β-alaO-*i*-Pr·HCl in the tracer experiment (see below). Clearly carbonate provides a route to opening the ester chelate without hydrolysis, with $[Co(en)_2(OH)(\beta\text{-alaO-}i\text{-Pr})]^{2+}$ subsequently reacting to form $[Co(en)_2(OCO_2)(\beta\text{-alaO-}i\text{-Pr})]^+$ under the conditions.

Table XIV gives the division of products (eq 13) for different experimental conditions. The increase in $[Co(en)_2(OH)(\beta$-

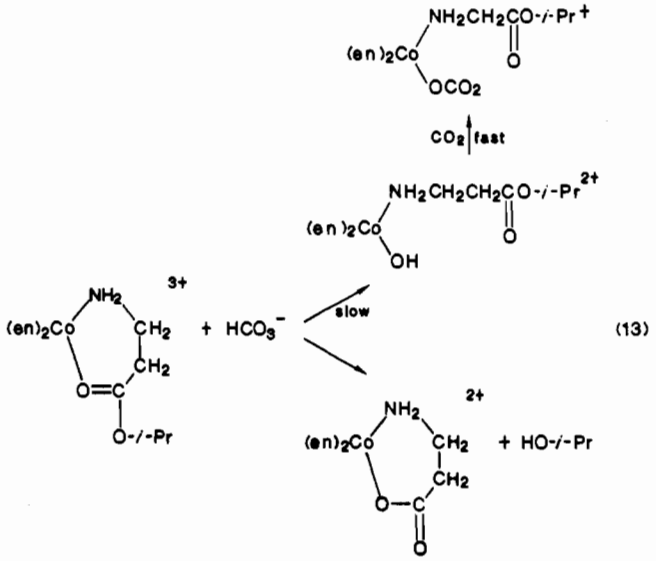

(13)

(10) Baraniak, E. Ph.D. Thesis, Australian National University, 1973.

Table XI. Molar Rotations (deg mol^{-1} dm^3 m^{-1}) of Products from the Acid (3 mol dm^{-3} HCl) and Alkaline (pH 10.62, 0.2 mol dm^{-3} NEt_3 Buffer) Hydrolyses of $(+)_{589}$-*cis*-$[Co(en)_2(OH_2/OH)(\beta\text{-alaO-}i\text{-Pr})]^{3+,2+}$

	$[Co(en)_2(\beta\text{-alaO})]^{2+}$			*cis*-$[Co(en)_2(OH)(\beta\text{-alaO})]^{+}$ [a]		
exptl cond[b]	589 nm	546 nm	436 nm	589 nm	546 nm	436 nm
3 mol dm^{-3} HCl	+920	+1480	−1710			
3 mol dm^{-3} HCl (2 mol dm^{-3} $NaClO_4$, neutral)	+920	+1260	−1300			
pH 10.62 (2 mol dm^{-3} $NaClO_4$, neutral)	+920	+1270	−1240	+910	+1240	−1200

[a] Analyzed following conversion to $[Co(en)_2(\beta\text{-alaO})]^{2+}$ at pH ~2. [b] See text.

Table XIII. Buffer Catalysis of Cyclization of *cis*-$[Co(en)_2(OH)(\beta\text{-alaO-}i\text{-Pr})]^{2+}$ in Aqueous Solution (25.0 °C, I = 1.0 ($NaClO_4$))

catalyst	pK_a	k_B, mol^{-1} dm^3 s^{-1}
OH^-	15.7	0.13
piperidine	11.4	1.3×10^{-3}
PO_4^{3-}	11.2	0.36
Et_3N	10.7	0.00
ethanolamine	9.7	1.8×10^{-4}
CO_3^{2-}	9.6	0.12
diethanolamine	9.15	1×10^{-4}
morpholine	8.9	1.7×10^{-4}
triethanolamine	8.13	2×10^{-5}
N-methylmorpholine	7.9	3.2×10^{-5}
Hepes	7.6	3×10^{-5}
H_2O	−1.7	1×10^{-7}

Table XIV. HCO_3^--Catalyzed Ring Opening of $[Co(en)_2(\beta\text{-alaO-}i\text{-Pr})]^{3+}$ (I = 1.0 ($NaClO_4$), 25.0 °C)

pH	$[CO_3]_T$, mol dm^{-3}	$[HCO_3^-]$, mol dm^{-3}	% $[Co(en)_2(OH)(\beta\text{-alaO-}i\text{-Pr})]^{2+}$ [b]
11.56	1.0	0	0
9.61	1.0	0.5	17
9.13	1.0	0.75	28
8.73	1.0	0	38
7.94	1.0	1.0	39
7.98	1.0	1.0	39
8.0[a]	0.5	0.5	38
8.0[a]	0.25	0.25	34
8.0[a]	0.25	0.25	33
8.0[a]	0.125	0.125	26
8.0[a]	0.125	0.125	26
8.0[a]	0.0625	0.0625	16
7.52–7.62[c]	1.0	~1.0	30
7.42–7.68[c]	1.0	~1.0	29

[a] pH and ionic strength maintained with 0.2 mol dm^{-3} Tris buffer. [b] IE chromatography and spectrophotometric analysis at 490 nm. [c] $[CO_3]_T$ buffer prepared by adding 1.0 mol dm^{-3} $HClO_4$ to a rapidly stirred solution of 1.0 mol dm^{-3} $NaHCO_3$ and immediately using.

alaO-*i*-Pr)]$^{2+}$ at constant total carbonate but decreasing pH implies HCO_3^- rather than CO_3^{2-} is the responsible reagent, and this is confirmed by the rate studies below. Furthermore, a saturation effect is apparent with little increase in $[Co(en)_2(OH_2)(\beta\text{-alaO-}i\text{-Pr})]^{3+}$ above 0.25 mol dm^{-3} HCO_3^- at pH 8.0. This implies that HCO_3^- catalyzes the formation of both $[Co(en)_2(OH)(\beta\text{-alaO-}i\text{-Pr})]^{2+}$ and $[Co(en)_2(\beta\text{-alaO})]^{2+}$ in the ratio ~2:3. Such division shows little pH dependence below pH 8. Separation of $[Co(en)_2(OH_2)(\beta\text{-alaO-}i\text{-Pr})]^{3+}$ from $[Co(en)_2(\beta\text{-alaO})]^{2+}$ in an experiment using carbonyl-^{18}O-labeled $[Co(en)_2(\beta\text{-alaO-}i\text{-Pr})]^{3+}$ and the removal of β-alaO-*i*-Pr by electrolysis (Table V, experiment 6) shows complete loss of label in the monodentate ester. The accompanying $[Co(en)_2(\beta\text{-alaO})]^{2+}$ however retains 93% of the label (Table V, experiment 7). Clearly C=O bond fission is involved in the former process and C—O-*i*-Pr bond fission in the latter (eq 13).

Rate data are given in Table III (supplementary data) and as plots of k_{obsd} vs. $[HCO_3^-]$ in Figure 6. Expression 14 represents the observed contribution to catalysis by HCO_3^-, with $k = 4 \times 10^{-2}$ mol^{-1} dm^3 s^{-1} and $K = 0.35$ mol^{-1} dm^3.

$$k_{obsd} - k_{aq} = \frac{k[HCO_3^-]}{1 + K[HCO_3^-]} \qquad (14)$$

Table XV. Kinetic Data for CO_2 Uptake by *cis*-$[Co(en)_2(OH)(\beta\text{-alaO-}i\text{-Pr})]^{2+}$ (25 °C, I = 1.0 ($NaClO_4$))[a]

$[HCO_3^-]$, mol dm^{-3}	pH	k_{obsd}, s^{-1}	$10^3[CO_2]$,[b] mol dm^{-3}	$k_{obsd}/[CO_2]$, mol^{-1} dm^3 s^{-1}
0.109	8.22	0.413	0.70	590
0.217	8.22	0.882	1.39	634
0.325	8.22	1.29	2.09	617
0.433	8.22	1.64	2.78	590
0.109	8.03	0.580	1.08	537
0.217	8.03	1.25	2.15	581
0.325	8.03	1.80	3.22	559
0.433	8.03	2.24	4.29	522

[a] Solutions were 0.1 mol dm^{-3} in Tris buffer and contained micromolar quantities of carbonic anhydrase to ensure maintenance of the CO_2–HCO_3^- equilibrium. $[Co]_T = 1 \times 10^{-4}$ mol dm^{-3}, λ = 310 nm. [b] Calculated with $pK_{CO_2(aq)} = 6.03$.[15]

Table XVI. Alkaline Hydrolysis of β-Alanine Esters (25.0 °C, I = 1.0 ($NaClO_4$))

ester	pH	$10^4 k_{obsd}$, s^{-1}	$k_{obsd}/[OH^-]$,[a] mol^{-1} dm^3 s^{-1}
$NH_2CH_2CH_2CO_2Me$	10.53	1.26	0.22
$NH_2CH_2CH_2CO_2$-*i*-Pr	11.61	1.56	0.021
	11.60	1.57	0.023
	12.84	21	0.018

[a] Calculated with pK_w = 13.77.

Scheme I

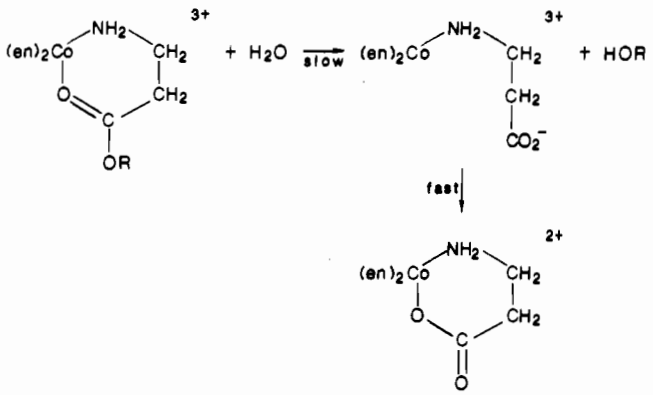

***cis*-$[Co(en)_2(OH)(\beta\text{-alaO-}i\text{-Pr})]^{2+}$ + CO_2.** The above rates for the HCO_3^--catalyzed reaction of the chelate were monitored by following the large absorbance change at 310 nm due to the formation of *cis*-$[Co(en)_2(OCO_2)(\beta\text{-alaO-}i\text{-Pr})]^+$ from one of the products, *cis*-$[Co(en)_2(OH)(\beta\text{-alaO-}i\text{-Pr})]^{2+}$ (eq 13). This reaction was followed separately (eq 15), and rate data given in Table XV fit expression 16 with $k_{CO_2} = 580 \pm 60$ mol^{-1} dm^3 s^{-1} (25.0 °C, I = 1.0 ($NaClO_4$)). Expression 16 agrees with that found for other hydroxo–Co(III) complexes in aqueous HCO_3^-,[15] and under the pH conditions used here there is no need to allow for the reverse hydrolysis reaction. *cis*-$[Co(en)_2(OCO_2)(\beta\text{-alaO-}i\text{-Pr})]ClO_4$ was also isolated and characterized. It is clear that this reaction is considerably faster than that for the chelate in the presence of

cis-$[Co(en)_2(OH)(\beta\text{-alaO-}i\text{-Pr})]^{2+}$ + CO_2 →
cis-$[Co(en)_2(OCO_2)(\beta\text{-alaO-}i\text{-Pr})]^+$ + H^+ (15)

$$k_{obsd} = k_{CO_2}[CO_2] \qquad (16)$$

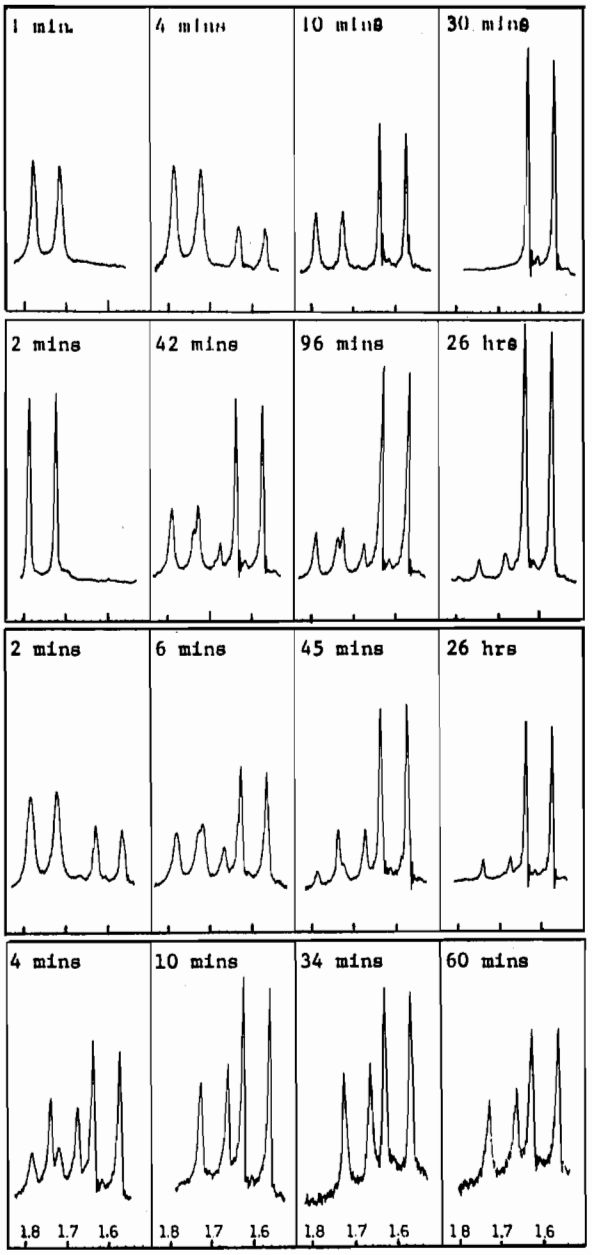

Figure 5. ^{1}H NMR spectra (100 MHz) of the isopropyl region during the hydrolysis of $[Co(en)_2(\beta\text{-alaO-}i\text{-Pr})]^{3+}$ in (a) 0.2 mol dm^{-3} collidine buffer, pD ~8, (b) collidine buffer containing a trace of added $NaHCO_3$, (c) collidine buffer containing approximately equimolar $NaHCO_3$, and (d) collidine buffer containing excess $NaHCO_3$ showing the growth and subsequent slow decay of the intermediate species $[Co(en)_2(OCO_2)(\beta\text{-alaO-}i\text{-Pr})]^+$ at ~1.7 ppm.

HCO_3^-, so that $k_{obsd} - k_{aq}$ of eq 14 is a measure of the HCO_3^--catalyzed opening of the chelate ring.

Free-Ligand Hydrolysis. Table XVI details kinetic data for hydrolysis of β-alanine esters (R = Me, *i*-Pr) under alkaline conditions. The pK_a for the isopropyl ester was measured as 9.43 ± 0.05 (25.0 °C, I = 1.0 ($NaClO_4$)). This value can be compared to 9.06 for the ethyl ester at I = 0.10.[11] The kinetic data support a first-order $[OH^-]$ dependence (eq 17), with k_{OH} = 2.0 × 10^{-2} mol^{-1} dm^3 s^{-1} for R = *i*-Pr and 2.2 × 10^{-1} mol^{-1} dm^3 s^{-1} for R = Me. The latter value is about twice that obtained by Hay and Morris at I = 0.1.[12]

$$NH_2CH_2CH_2CO_2R + OH^- \rightarrow NH_2CH_2CH_2CO_2^- + ROH \quad (17)$$

(11) Perrin, D. D. In *Dissociation Constants of Organic Bases in Aqueous Solution*; Butterworths: London, 1965.
(12) Hay, R. W.; Morris, P. J. *J. Chem. Soc. B* **1970**, 1577.

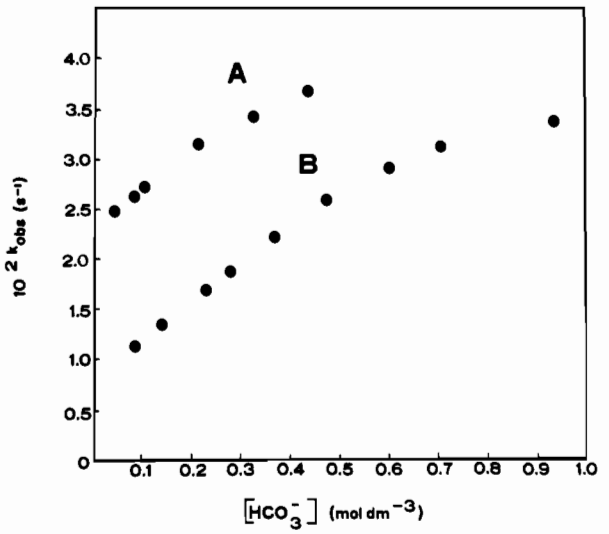

Figure 6. k_{obsd} vs. $[HCO_3^-]$ rate profile for the HCO_3^--catalyzed reaction of $[Co(en)_2(\beta\text{-alaO-}i\text{-Pr})]^{3+}$ (I = 1.0 ($NaClO_4$), 25.0 °C). Upper points are data obtained at pH 8.22; lower points are data obtained at pH 7.97.

Scheme II

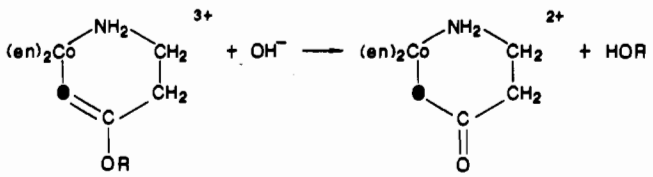

Discussion

Hydrolysis of $[Co(en)_2(\beta\text{-alaO-}i\text{-Pr})]^{3+}$. Hydrolysis of the directly activated ester in acid solution occurs without opening of the chelate ring and without specific H^+ or general-acid catalysis. No ring-opened species such as $[Co(en)_2(OH_2)(\beta\text{-alaO-}i\text{-Pr})]^{3+}$ or $[Co(en)_2(OH_2)(\beta\text{-alaO})]^{2+}$ are formed; such species have properties that would allow their detection. This does not exclude simultaneous ring opening and hydrolysis followed by ring closure in a five-coordinate intermediate (Scheme I) but such a result is extremely unlikely and would require the exclusive reentry of carboxylate. The substantial amounts of Co–OH_2 species formed in closely related induced reactions of Co(III) complexes in acid solution (e.g. in the Hg^{2+}-induced reaction of *cis*-$[Co(en)_2Br(\beta\text{-alaO})]^+$[7]) argue strongly against any detachment of the ester function from the metal during hydrolysis. The absence of additional specific H^+ or general acid catalysis is accounted for by the metal assuming this role. Compared to the uncoordinated ester the activation provided by the metal is substantial but a direct estimate is uncertain due to the slowness of the uncatalyzed reaction of the uncoordinated ester. For glycine esters, which involve five-membered chelates and possibly slightly more activation due to chelate ring strain, an acceleration of ~10^5 is involved. Table XVII gives some comparative rate data.

In alkaline solution attachment of the ester function to the metal throughout hydrolysis is established by the ^{18}O tracer results. A distinction between the nucleophile and ester O atoms is also demonstrated, and the expected acyl–OR bond cleavage occurs (Scheme II).

The pH rate profile, Figure 3, provides new information on metal-catalyzed ester hydrolysis. The two clear inflections require at least one change in rate-determining step and at least one

(13) Sutton, P. A.; Buckingham, D. A., unpublished data.
(14) Buckingham, D. A.; Foster, D. M.; Sargeson, A. M. *J. Am. Chem. Soc.* **1969**, *91*, 3451.
(15) Chaffee, E.; Dasgupta, T. P.; Harris, G. M. *J. Am. Chem. Soc.* **1973**, *95*, 4169.
(16) Miskelly, G. M.; Buckingham, D. A.; Clark, C. R., submitted for publication in *J. Am. Chem. Soc.*
(17) Boreham, C. J.; Buckingham, D. A.; Keene, F. R. *J. Am. Chem. Soc.* **1979**, *101*, 1409.

Table XVII. Comparisons of Rate Constants for Hydrolysis of Chelated and Monodentate Glycine and β-Alanine Isopropyl Esters at 25 °C

substrate, nucleophile	rate[a]	comments
$H_3^+NCH_2CO_2$-*i*-Pr + H_2O	$\sim 2 \times 10^{-11}$	estimated as 5 times slower than ethyl ester[c]
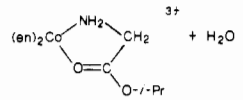	2.0×10^{-5} [d]	addition of H_2O probably rate determining
$H_3^+NCH_2CH_2CO_2$-*i*-Pr + H_2O	$\sim 2 \times 10^{-12}$	estimated as 10 times slower than glycine ester
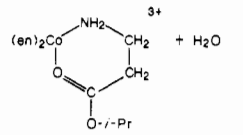	8.3×10^{-7} [e]	addition of H_2O probably rate determining
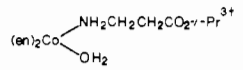	1.8×10^{-6} [b,e]	addition of coordinated H_2O rate determining
$H_2NCH_2CO_2$-*i*-Pr + OH^-	0.2[f]	
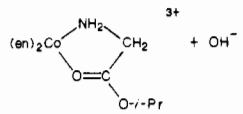	1.5×10^{6} [g]	elimination of *i*-PrO^- probably rate determining
$H_2NCH_2CH_2CO_2$-*i*-Pr + OH^-	0.02[e]	
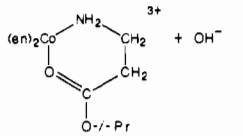	4×10^{4} [e]	addition of OH^- rate determining for pH >10, otherwise elimination of *i*-PrO^- rate determining
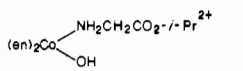	fast[h]	rate not observed
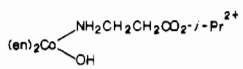	5.6×10^{-6} [b,e]	addition of coordinated OH^- rate determining
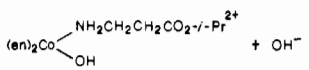	0.13[e]	addition of coordinated OH^- rate determining

[a] Units of mol^{-1} dm^3 s^{-1} unless otherwise indicated. [b] Units of s^{-1}. [c] Conley, H. L.; Martin, R. B. *J. Phys. Chem.* **1965**, *69*, 2914. [d] Reference 8. [e] This work. [f] Hay, R. W.; Porter, L. J.; Morris, P. J. *Aust. J. Chem.* **1960**, *19*, 1197. A factor of 5 slower for R = *i*-Pr vs. R = Et. [g] Reference 2. [h] Reference 5.

intermediate, although the latter need not be directly related to hydrolysis. Deprotonation of a coordinated amine center by OH^- may be considered since H exchange at such sites is very rapid under the alkaline conditions.[18] However, the high pK_a of such sites (≥14) would not generate the observed rate profile, and such deprotonations usually result in hydrolysis at the metal center rather than at a ligand site. Deprotonation at the α-carbon adjacent to the ester function is another possibility, and this does occur competitively in the related chelated glycine esters under the present mild pH conditions.[13] But it can be eliminated here since integration of the 2.8–3.5-ppm region of Figure 1A, and its hydrolysis product at pD ~9, shows that no C–H exchange has occurred. The kinetic data are accommodated by a stepwise addition–elimination mechanism in which addition of OH^- to the acyl-activated ester is followed by loss of RO^- from an intermediate by OH^--independent and OH^--dependent paths. At low pH (<7.5) OH^--independent elimination is rate-determining, at intermediate pHs (8–10.0) OH^--dependent elimination takes over, while OH^- addition to the ester is rate-determining above pH 10. Two possibilities exist for the elimination process, and these are given by Schemes III and IV. Either proton abstraction from IH is rate-determining (Scheme III) or it is not (Scheme IV). Scheme III leads to the rate expression

$$\frac{-d[Co(ester)]}{dt} = \frac{k_1k_2[OH^-] + k_1k_3[OH^-]^2}{k_{-1} + k_2 + k_3[OH^-]}[Co(ester)] \quad (18)$$

(18) Figure 1B shows the almost absence of the broad NH resonances at 4.7 and 5.5–6.5 ppm (Figure 1A,C), which characterize the coordinated amine protons. Thus, substantial NH exchange has occurred at the amine sites in neutral D_2O in the time taken to prepare and run the spectrum. NH absorptions are immediately absent in alkaline solution.

and comparisons with the observed data at pH >10, pH <8, and 8 < pH < 10, respectively, lead to

$$k_1 = 4.0 \times 10^4 \text{ mol}^{-1} \text{ dm}^3 \text{ s}^{-1} \quad (19)$$

$$\frac{k_2}{k_{-1} + k_2} = 0.125 \quad (20)$$

$$\frac{k_3}{k_{-1} + k_2} = 1.75 \times 10^4 \text{ mol}^{-1} \text{ dm}^3 \quad (21)$$

with

$$k_{-1}/k_2 = 7 \quad (22)$$

Comparison of (20) with (21) gives $k_3/k_2 = 10^5$ mol^{-1} dm^3, and a comparison of k_{obsd} in H_2O and D_2O at high pH leads to $k_1(OH)/k_1(OD) = 0.74$ and at low pH to little isotope dependence for the $k_2/(k_{-1} + k_2)$ division. The latter two results are in agreement with OD^- being the better nucleophile and with the transition state occurring early in the addition process. This mechanism does not distinguish rate-determining proton abstraction with fast subsequent loss of RO^- from base conjugate I from concerted deprotonation and loss of RO^- without formation of an identifiable intermediate I. We favor the former, largely on grounds that metal ions appear to prefer stepwise processes.[9] The reasons for this are at present not entirely clear but may be associated with the properties of saturated and unsaturated chelate ring systems.

The alternative possibility involving fast equilibrium deprotonation of IH and rate-determining loss of RO^- from I (Scheme

Scheme III

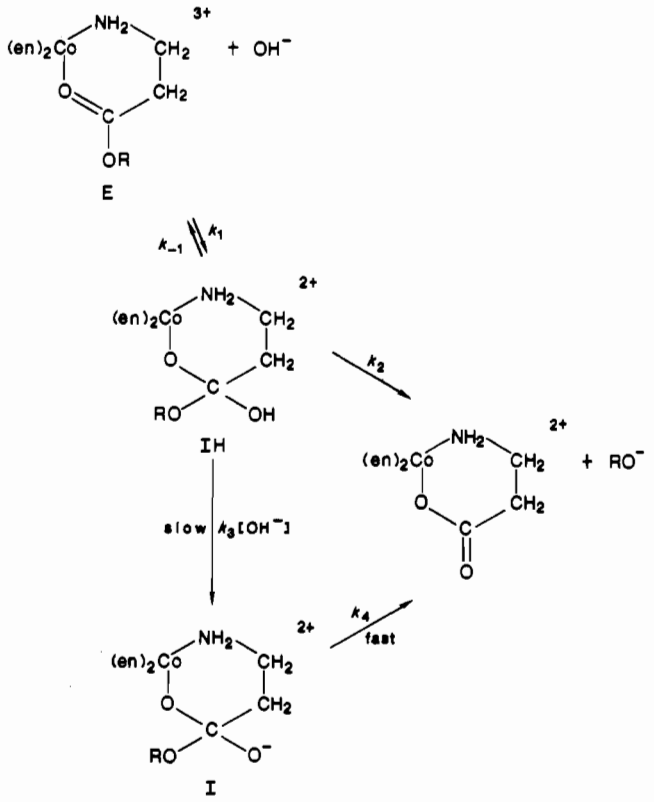

Scheme IV

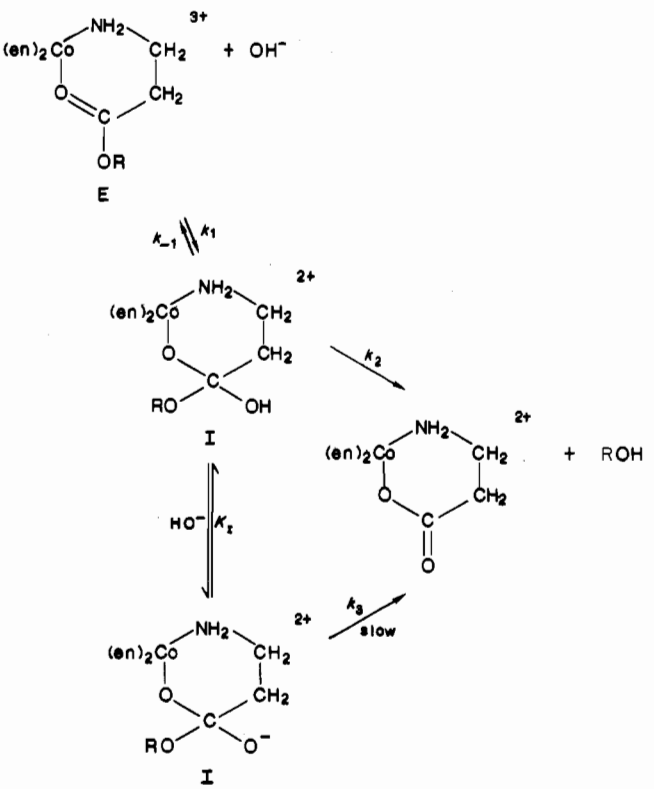

IV) arises only as a result of the absence of observed general-base catalysis in the decomposition of IH. If terms of the form k-$[OH^-][B]$ were present ($B \neq OH^-$) in the rate at pHs <8, then this possibility would not arise. Scheme IV leads to the rate expression

$$\frac{-d[Co(ester)]}{dt} = \frac{k_1k_2[OH^-] + k_1k_3K_I[OH^-]^2}{k_2 + k_{-1} + k_3K_I[OH^-]}[Co(ester)] \quad (23)$$

and comparisons with the observed data (eq 7) give

$$k^I = \frac{k_1k_2}{k_{-1} + k_2} = 5.0 \times 10^3 \text{ mol}^{-1} \text{ dm}^3 \text{ s}^{-1} \quad (24)$$

$$k^{II} = \frac{k_1k_3K_I}{k_2 + k_{-1}} = 7.0 \times 10^8 \text{ mol}^{-2} \text{ dm}^6 \text{ s}^{-1} \quad (25)$$

$$K = \frac{k_3K_I}{k_2 + k_{-1}} = 1.75 \times 10^4 \text{ mol}^{-1} \text{ dm}^3 \quad (26)$$

whence $k_1 = 4.0 \times 10^4$ mol^{-1} dm^3 s^{-1}, $k_2/(k_2 + k_{-1}) = 0.125$, and $k_{-1}/k_2 = 7$, as before. The latter ratio gives the preferred loss of HO^- compared to i-PrO^- from IH and is in line with their known basicities. An estimate of K_I may be obtained by considering the polarizing effect of Co(III) on IH. Electron-withdrawing groups considerably enhance the acidity of alcohols, viz. CCl_3CH_2OH ($pK_a = 12.44$) and CF_3CH_2OH (12.37), and hemiketals are expected to be of similar acidity to their more accessible *gem*-diol analogues, $HCH(OH)_2$ (13.27), $CH_3CH(OH)_2$ (13.57), $CF_3C(CH_3)(OH)_2$ (10.44), and $CF_3C(m\text{-}NO_2C_6H_4)C(OH)_2$ (9.18). The effect of replacing H^+ by Co(III) in such species may be approximated by comparing $HOCO_2H$ with $[(NH_3)_5Co(OCO_2H)]^{2+}$. The pK_a's of 3.9 for the former and 6.4 for the latter suggest that Co(III) is a poor substitute for H^+ in this situation. The pK_a of IH might therefore be expected to be in the vicinity of 14, whence $K_I \cong 1$ mol^{-1} dm^3. This leads to

$$\frac{k_1k_2}{k_3} = 0.4 \text{ mol}^{-1} \text{ dm}^3 \text{ s}^{-1} \quad (27)$$

with

$$\frac{k_3}{k_2} \cong 10^5 \quad (28)$$

That is, RO^- is a 10^5 times better leaving group from oxyanion I than it is from its conjugate acid IH.

The question of rate-determining proton abstraction or loss of RO^- deserves further comment. In the related aminolysis reaction deprotonation of INH by bases other than OH^- is observed,[9] and

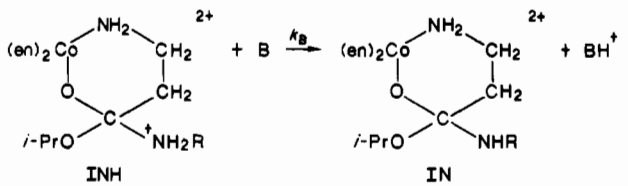

this part of the reaction must therefore be rate-determining. There the acidity of INH is increased (estimated $pK_a = 7$)[9] compared to IH ($pK_a \sim 14$) so that general-base catalysis is more expected.[19] Also, the Brønsted coefficient of ~0.65 in the aminolysis reaction implies that deprotonation is a major contributor to this activation process with little contribution from the loss of RO^-. It is expected that for the poorer acid IH considered here a similar situation obtains, and the absence of terms of the type $k[OH^-][B]$ for $B \neq OH^-$ may merely mean the other bases are not sufficiently basic to compete with OH^- for proton abstraction from this intermediate under the experimental conditions. For this reason Scheme III is preferred over Scheme IV with specific OH^--catalyzed rate-determining proton abstraction. If loss of RO^- occurs in concert (that is if I is not a true intermediate), then the absence of HO^--catalyzed ^{18}O exchange into the product chelated acid under the same conditions argues for an early transition state for the loss of RO^-. Similar specific OH^--catalyzed loss of RO^- has been found with VIII.[14]

Apart from HCO_3^- and HPO_4^{2-}, buffer-catalyzed hydrolysis (Table IV) is of minor importance compared to the OH^--induced reaction. The absence of terms $k[OH^-][B]$ for imidazole and

(19) Jencks, W. P. In *Catalysis in Chemistry and Enzymology*; McGraw-Hill: New York, 1969.

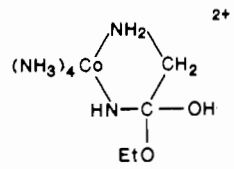

VIII

N-methylimidazole eliminates them as contributing to the OH^--induced deprotonation of IH. Loss of RO^- is rate-determining at these pHs. Nucleophilic addition of these bases would lead to IX, in which imidazole is easily the best leaving group,

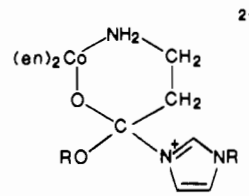

IX

so that such a process would be unproductive. The absence of a $k[Im][OH^-]$ term also removes the possibility of deprotonation of the imidazole species (IX) leading to loss of RO^- and subsequent rapid hydrolysis of $[Co(en)_2(\beta\text{-ala-Im})]^{3+}$. With glycine ethyl ester a $k[OH^-][GlyOEt]$ contribution to the rate does occur,[9] but this results in the OH^--catalyzed formation of the amide $[Co(en)_2(\beta\text{-ala-glyOEt})]^{3+}$ via INH. We suggest that catalyzed hydrolysis by these amine bases results from general-base-catalyzed addition of water (Scheme V). A similar role is envisaged for the more marked catalysis by HPO_4^{2-} and HCO_3^- (Table IV). Again, the absence of $k[B][OH^-]$ terms (CO_3^{2-} and PO_4^{3-} not catalyzing the reaction) removes the possibility of HPO_4^{2-} or HCO_3^- catalyzing the deprotonation of IH following OH^- addition, and the rates of hydrolysis at the highest HPO_4^{2-} concentrations are faster than those for the uncatalyzed addition of OH^- (extrapolated k_1 values) at these pHs. Such observations require a concerted low-energy path, and the ability of these buffers to act as proton donors as well as acceptors provides a route to products that avoids IH. Scheme VI outlines this "proton switch"[24] proposal. With HCO_3^-, no rapidly formed intermediate was observed in stopped-flow traces (310 nm), and ^1H NMR spectra (Figure 5) showed the presence of only unreacted chelate and the two products $[Co(en)_2(\beta\text{-alaO})]^{2+}$ and *cis*-$[Co(en)_2(OCO_2)(\beta\text{-alaO-}i\text{-Pr})]^+$ during the reaction. However, whereas HPO_4^{2-} catalyzes only hydrolysis, HCO_3^- provides alternate modes of acyl cleavage, one in the chelate ring (ester O exchange) and the other external to it (hydrolysis). The former cleavage pattern is unique in our experience, although O exchange in uncoordinated esters undergoing hydrolysis has been extensively studied by others.[20-22] Cleavage of a chelate ring at a non metal position is uncommon and to our knowledge has been found previously only with five-membered oxalate.[16,23]

Hydrolysis of *cis*-$[Co(en)_2(OH_2/HO)(\beta\text{-alaO-}i\text{-Pr})]^{3+/2+}$. Although not unrelated to hydrolysis of the chelated ester the initial aspects of this reaction are considered separately. In acid the monodentate aqua ester $[Co(en)_2(OH_2)(\beta\text{-alaO-}i\text{-Pr})]^{3+}$ slowly cyclizes and hydrolyzes ($k_4 = 1.8 \times 10^{-6}\ s^{-1}$), and the tracer results give clear evidence for intramolecular attack by the coordinated aqua ligand at the acyl center (Scheme VII). The tracer data also give some measure of exchange into the reactant ($k_{ex} = 1.5 \times 10^{-5}\ s^{-1}$). Although not an unreasonable result, this latter value is some 10 times greater than that reported for *cis*-$[Co(en)_2(OH_2)(NH_3)]^{3+}$ ($k_{ex} = 1.1 \times 10^{-6}\ s^{-1}$, 25.0 °C).[25] Loss of label

Scheme V

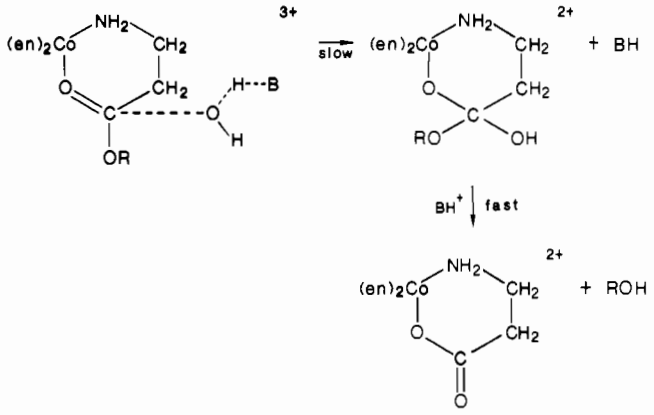

Scheme VI

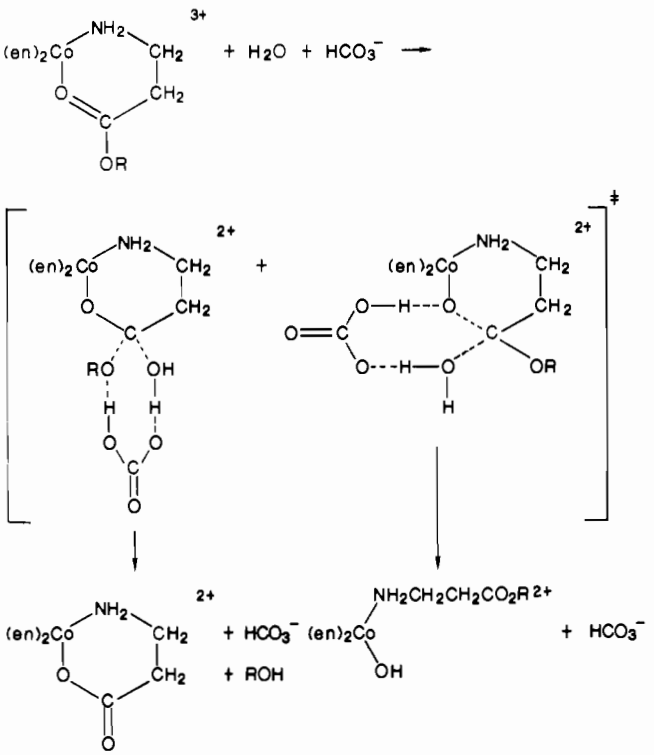

Scheme VII

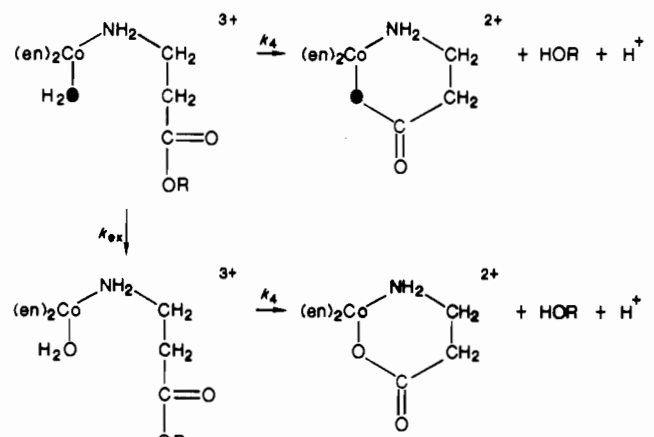

(20) (a) Bender, M. L. *J. Am. Chem. Soc.* **1951**, *73*, 1626–1629. (b) Bender, M. L.; Thomas, R. J. *Ibid.* **1961**, *83*, 4183–4189. (c) Bender, M. L.; Thomas, R. J. *Ibid.* **1961**, *83*, 4189–4193. (d) Bender, M. L.; Heck, H. d. *Ibid.* **1967**, *89*, 1211–1220.
(21) (a) Shain, S. A.; Kirsch, J. F. *J. Am. Chem. Soc.* **1968**, *90*, 5848–5854. (b) Sawyer, C. B.; Kirsch, J. F. *Ibid.* **1973**, *95*, 7375–7386.
(22) (a) O'Leary, M. H.; Marlier, J. F. *J. Am. Chem. Soc.* **1979**, *101*, 3300–3306. (b) Marlier, J. F.; O'Leary, M. H. *J. Org. Chem.* **1981**, *46*, 2175–2177.
(23) Andrade, C. A.; Taube, H. *J. Am. Chem. Soc.* **1964**, *86*, 1328.
(24) Hogg, L. J.; Jencks, D. A.; Jencks, W. P. *J. Am. Chem. Soc.* **1977**, *99*, 4772.

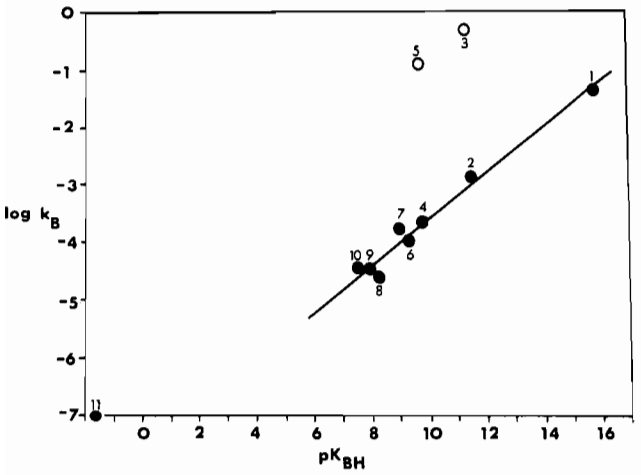

Figure 7. Brønsted plot of log k_B vs pK_{BH} for the general base-catalyzed cyclization of *cis*-$[Co(en)_2(OH)(\beta\text{-alaO-}i\text{-Pr})]^{2+}$ to $[Co(en)_2(\beta\text{-alaO})]^{2+}$: 1, OH^-; 2, piperidine; 3, PO_4^{3-}; 4, ethanolamine; 5, CO_3^{2-}; 6, diethanolamine; 7, morpholine; 8, triethanolamine; 9, *N*-methylmorpholine; 10, HEPES; 11, H_2O.

in the isolation procedure or in the generation of CO_2 could account for this difference. However, the 71% incorporation of label into the chelate after 10% reaction (Table V) establishes that k_4 represents attack by coordinated water in an uncatalyzed process. In this case proton transfer in the transition state undoubtedly plays an important role. Rapid cyclizations have been observed previously with $[Co(en)_2(OH_2)(glyOH)]^{3+}$ ($t_{1/2} \sim 40$ s),[27] $[Co(en)_2(OH_2)(glyO)]^{2+}$ ($t_{1/2} \sim 400$ s),[27] and $[Co(en)_2(OH_2)(glyNH_2)]^{3+}$ ($t_{1/2} \sim 75$ s).[17] In these previous examples the acyl center would be expected to be more resistant to attack by coordinated water than in the monodentate ester. However, the intramolecular nature of these reactions is important with the five-membered chelates being formed more rapidly than the present six-membered chelate. Coordinated water is undoubtedly a poorer nucleophile than solvated water in a bimolecular sense, and no examples of $Co\text{–}OH_2^{3+}$ additions or hydrolyses are known for separated reactants.

In alkaline solution the rate data (Figure 4) clearly require both OH^--assisted and unassisted hydrolysis for the hydroxo complex $[Co(en)_2(OH)(\beta\text{-alaO-}i\text{-Pr})]^{2+}$. The pK_a of 6.05 for the aqua ligand results in some uncertainty as to the interpretation of the unassisted reaction (i.e. OH^--catalyzed cyclization of the aqua complex is possible), but the involvement of bases other than OH^- (Table XIII) supports it being viewed as unassisted or solvent-assisted cyclization of $[Co(en)_2(OH)(\beta\text{-alaO-}i\text{-Pr})]^{2+}$. Figure 7 gives a Brønsted plot of log k_B (eq 12, including k_{OH}, and Table XIII) vs. pK_a. With the exception of H_2O, PO_4^{3-}, and CO_3^{2-} the good linear correlation ($\beta \approx 0.4$) supports appreciable involvement of the catalyzing base in the transition state. The tracer data (Table V) clearly require intramolecular attack by coordinated hydroxide at the acyl site (Scheme VIII) for the k_{OH} term, and the correlation given by Figure 7 supports this in a general sense.

The intramolecular nature of the reaction is again important. $Co\text{–}OH^{2+}$ is $\sim 10^4$ times less effective than HO^- in hydrolyzing (*p*-nitrophenyl)acetate in a simple bimolecular reaction,[26] and extrapolation of such correlations[26] gives a rate of $\sim 10^{-8}$ mol^{-1} dm^3 s^{-1} for the hydrolysis of β-alaO-*i*-Pr by $Co\text{–}OH^{2+}$. The value of 0.13 mol^{-1} dm^3 s^{-1} found here (Table XIII) represents a 10^7-fold enhancement. The particular ability of PO_4^{3-} and CO_3^{2-} (Figure 7) suggests a special property for these bases. This could be direct transfer of the proton to the alcohol function, thereby avoiding intermediate IH of Scheme VIII, that is, a concerted addition–elimination process rather than a stepwise reaction. But these catalysts are not normally classed as "proton switch" species.[24]

(25) Martin, D. F.; Tobe, M. L. *J. Chem. Soc.* **1962**, 1388.
(26) Buckingham, D. A.; Clark, C. R. *Aust. J. Chem.* **1982**, *35*, 431.
(27) Boreham, C. J.; Buckingham, D. A.; Francis, D. J.; Sargeson, A. M.; Warner, L. G. *J. Am. Chem. Soc.* **1981**, *103*, 1975.

Scheme VIII

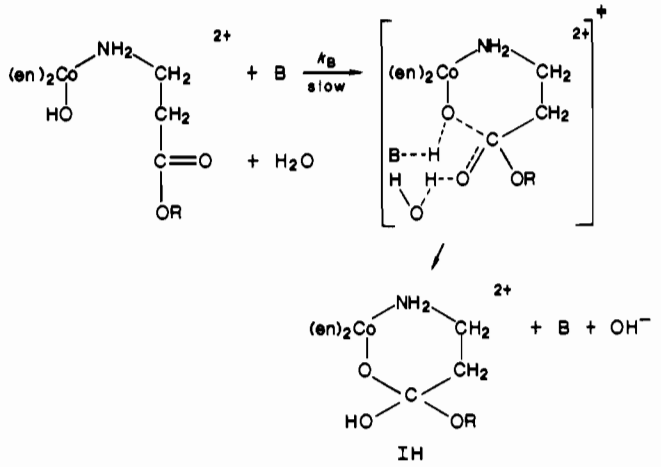

Scheme IX

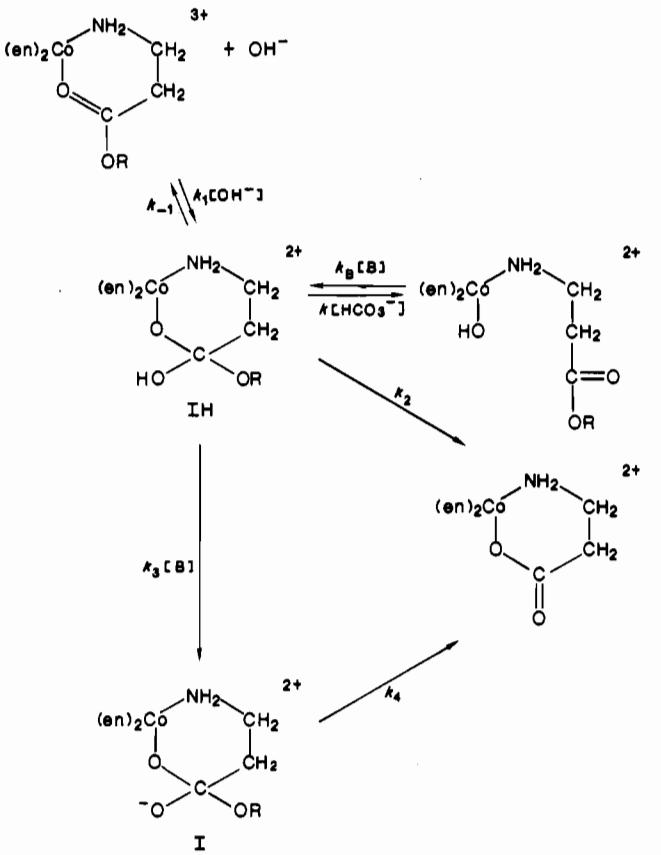

The involvement of IH in the OH^--catalyzed reaction is clearly demonstrated by the trapping experiments in the presence of glycine ethyl ester. The formation of chelated amide, $[Co(en)_2(\beta\text{-ala-glyOEt})]^{3+}$ (29% and 15% for 1.0 and 0.5 mol dm^{-3} glycine ester, respectively), requires the presence of chelated ester, and the k_{-1}/k_2 ratio of 7 found above gives the division of IH to chelated ester and hydrolyzed product under the pH 7.9 conditions of these experiments. Specifically, since only ~60% of the hydroxo monodentate ends up as cyclized product (the remainder resulting in *cis*- + *trans*-$[Co(en)_2(OH)(\beta\text{-alaO})]^+$, Table VIII), some $^6/_7 \times 60\% = 54\%$ $[Co(en)_2(\beta\text{-alaO-}i\text{-Pr})]^{3+}$ would result from a fully formed IH intermediate. It has been shown[9] that the chelated ester results in 60% and 43% $[Co(en)_2(\beta\text{-ala-glyOEt})]^{3+}$ under the two sets of conditions so that the derived results of 32.4% and 23% agree reasonably well with those observed. This means that intermediate IH is a common one for hydrolysis of both the chelated and monodentate ester complexes. Scheme IX summarizes these observations and gives an overall representation of the hydrolysis paths. Specific OH^--catalyzed proton loss from

IH to form I is preferred as the rate-determining step for the decomposition of IH under alkaline conditions, but this aspect remains uncertain.

Acknowledgment. We thank Dr. F. Bergersen and G. Turner of the Division of Plant Industry, CSIRO, Canberra, Australia, and Dr. J. Hulston of the Institute of Nuclear Sciences, DSIR, Lower Hutt, New Zealand, for carrying out the ^{18}O tracer measurements.

Registry No. $[Co(en)_2(\beta\text{-alaOMe})](ClO_4)_3$, 103477-77-6; $[Co(en)_2(\beta\text{-alaO-}i\text{-Pr})](ClO_4)_3$, 103477-73-2; *cis*-$[Co(en)_2(OH_2)(\beta\text{-alaO-}i\text{-Pr})](NO_3)_2(ClO_4)$, 103498-63-1; *cis*-$[Co(en)_2(OCO_2)(\beta\text{-alaO-}i\text{-Pr})]ClO_4$, 103477-79-8; *cis*-$[Co(en)_2Br(\beta\text{-alaOMe})]Br_2$, 101695-41-4; *cis*-$[Co(en)_2Br(\beta\text{-alaO-}i\text{-Pr})]Br_2$, 101695-40-3; *cis*-$[Co(en)_2(OH_2)(\beta\text{-alaO-}i\text{-Pr})](NO_3)_3$, 103477-81-2; *trans*-$[Co(en)_2(OH)(\beta\text{-alaO})]^+$, 103477-82-3; *cis*-$[Co(en)_2(OH)(\beta\text{-alaO})]^+$, 103531-54-0; $[Co(en)_2(\beta\text{-alaO})]^{2+}$, 63771-19-7; *trans*-$[Co(en)_2(OH_2)(\beta\text{-alaOH})]^{3+}$, 103477-83-4; *cis*-$[Co(en)_2(OH_2)(\beta\text{-alaOH})]^{3+}$, 103531-55-1; β-alaO-*i*-Pr, 39825-36-0; β-alaOMe, 4138-35-6; OH^-, 14280-30-9; PO_4^{3-}, 14265-44-2; Et_3N, 121-44-8; CO_3^{2-}, 3812-32-6; H_2O, 7732-18-5; HCO_3^-, 71-52-3; ethanolamine, 141-43-5; diethanolamine, 111-42-2; morpholine, 110-91-8; triethanolamine, 102-71-6; *N*-methylmorpholine, 109-02-4; Hepes, 7365-45-9; piperidine, 110-89-4.

Supplementary Material Available: Listings of rate data for the hydrolysis of $[Co(en)_2(\beta\text{-alaO-}i\text{-Pr})]^{3+}$ in alkaline solution (Table II), for buffer-catalyzed hydrolysis (Table III), for alkaline hydrolysis of *cis*-$[Co(en)_2(OH)(\beta\text{-alaO-}i\text{-Pr})]^{2+}$ (Table VII), and for buffer-catalyzed hydrolysis (Table XII) (12 pages). Ordering information is given on any current masthead page.

Contribution from the Department of Chemistry, University of Otago, Dunedin, New Zealand

Metal Ion Activated Aminolysis of Esters. Reaction of Glycine Ethyl Ester with $[Co(en)_2(\beta\text{-alaO-}i\text{-Pr})]^{3+}$ and General-Base-Catalyzed Decomposition of Metal Alcohol–Amine Intermediates

David A. Buckingham* and Charles R. Clark

Received February 18, 1986

The aminolysis of the Co(III)-chelated, acyl-activated, β-alanine isopropyl ester in $[Co(en)_2(\beta\text{-alaO-}i\text{-Pr})]^{3+}$ by glycine ethyl ester in aqueous solution follows the rate expression $k_{obsd} = k'[B] + k''[GlyOEt][B]$ with only the k'' terms resulting in the aminolysis product $[Co(en)_2(\beta\text{-ala-glyOEt})]^{3+}$; k' terms result in hydrolysis of the ester to give $[Co(en)_2(\beta\text{-alaO})]^{2+}$. k'' takes values 3.9×10^3 (B = HO^-), 3.5×10^{-2} (B = GlyOEt), and 2.9×10^{-2} (B = Im) $mol^{-2}\ dm^6\ s^{-1}$, and k', 5.0×10^3 (B = HO^-), 3×10^{-3} (B = GlyOEt) and 4.5×10^{-3} (B = Im) $mol^{-1}\ dm^3\ s^{-1}$, all at $I = 1.0$ (NaCl) mol dm^{-3} and 25.0 °C. The requirement for another catalyzing base to be present in the aminolysis reaction is interpreted as rate-determining deprotonation of an amine–alcohol intermediate. The properties of such metal addition intermediates are discussed.

Several years ago in a study of the O and N lysis of cobalt(III)-chelated glycine esters in aqueous solution we left unresolved mechanistic details of the aminolysis reaction.[1] It was shown that $[Co(en)_2(glyNHR)]^{3+}$ was formed from $[Co(en)_2(glyO\text{-}i\text{-}Pr)]^{3+}$ by first and second order in $[NH_2R]$ pathways, but the rates of reaction were too fast to establish a rate law from kinetic measurements. The possible rapid formation of an alcohol–amine intermediate that slowly lost RO^- or ROH via general-base- or general-acid-catalyzed processes was suggested but not proven. In another study using Me_2SO media, an addition intermediate was clearly identified and amine-catalyzed loss of ROH was established.[2]

By using the less reactive ester isopropyl β-alaninate chelated to Co(III), it has now been possible to examine the aminolysis reaction in aqueous solution in some detail. This paper reports its reaction with glycine ethyl ester to form the chelated dipeptide $[Co(en)_2(\beta\text{-ala-glyOEt})]^{3+}$. The form of the rate law and the characterization of the rate-determining step are expected to be general features in the aminolysis of all metal-activated esters. Hydrolysis of the same chelated ester is considered in an accompanying paper.[3]

Experimental Section

The preparation of $[Co(en)_2(\beta\text{-alaO-}i\text{-Pr})](ClO_4)_3$ has been described previously.[3] Imidazole was recrystallized from toluene and dried under vacuum, and glycine ethyl ester hydrochloride was twice recrystallized from methanol–ether. $[Co(en)_2(\beta\text{-ala-glyOEt})](ClO_4)_2(NO_3)\cdot H_2O$ was prepared as follows. To a solution of $[Co(en)_2(\beta\text{-alaO-}i\text{-Pr})](ClO_4)_3$ (1.217 g) and GlyOEtHCl (0.70 g) in dry Me_2SO (20 cm^3) was added Et_3N (0.303 g) and the mixture allowed to stand at room temperature for 10 min before dilution with water (200 cm^3). IE chromatography (Sephadex SP-C25) using NaCl eluent (0.2–0.5 mol dm^{-3}) resulted in the recovery of an orange 3+ band. This was reduced to dryness (rotary evaporator) and the product complex desalted by extracting into MeOH (20 cm^3), filtering, and evaporating to dryness. This procedure was repeated a further two times with MeOH–EtOH (1:1) being used in the final extraction. The orange product was dissolved in water (4 cm^3, 70 °C) and $LiNO_3$ (0.3 g) and $NaClO_4$ (0.4 g) added. On cooling, $[Co(en)_2(\beta\text{-ala-glyOEt})](ClO_4)_2(NO_3)\cdot H_2O$ crystallized. This was washed with EtOH and then Et_2O and air-dried. Anal. Calcd for $[CoC_{11}H_{30}N_6O_3](ClO_4)_2(NO_3)\cdot H_2O$: C, 20.90; H, 5.10; N, 15.51.

(1) Buckingham, D. A.; Foster, D. M.; Sargeson, A. M. *J. Am. Chem. Soc.* **1970**, *92*, 5701.
(2) Buckingham, D. A.; Dekkers, J.; Sargeson, A. M. *J. Am. Chem. Soc.* **1973**, *95*, 4173.
(3) Baraniak, E.; Buckingham, D. A.; Clark, C. R.; Moynihan, B. H.; Sargeson, A. M. *Inorg. Chem.*, preceding paper in this issue.
(4) Jencks, W. P. In *Catalysis in Chemistry and Enzymology*; McGraw-Hill: New York, 1969.
(5) Gravitz, N.; Jencks, W. P. *J. Am. Chem. Soc.* **1974**, *96*, 499.
(6) DeTar, D. F. *J. Am. Chem. Soc.* **1982**, *104*, 7205.
(7) At 310 and 495 nm with 0.5 mol dm^{-3} glycine ethyl ester buffer (pH 7.82, $I = 1.0$ (NaCl)), stopped-flow traces showed no evidence for an intermediate over the first few seconds of reaction.
(8) Knighton, D. R.; Harding, D. R. K.; Friar, M. J.; Hancock, W. S.; Reynolds, G. D.; Clark, C. R.; Tasker, R. F.; Buckingham, D. A. *J. Am. Chem. Soc.* **1981**, *103*, 7025.
(9) Hay, R. W.; Morris, P. J. *Met. Ions Biol. Syst.* **1976**, *5*, 174.
(10) Curtis, N. J.; Sargeson, A. M. *J. Am. Chem. Soc.* **1984**, *106*, 625 and references therein.
(11) Boreham, C. J.; Buckingham, D. A.; Keene, F. R. *J. Am. Chem. Soc.* **1979**, *101*, 1409.
(12) Jencks, W. P. *Chem. Soc. Rev.* **1981**, *10*, 345.

0020-1669/86/1325-3478$01.50/0